

1 RUNNING HEAD: CUE COMBINATION FOR SELF-LOCALIZATION

2

3

4 Cue Combination Used to Update the Navigator's Self-localization, not the Home Location

5

6 Lei Zhang, Weimin Mou\*, Xuehui Lei, Yu Du

7 University of Alberta

8

9 Author Note

10 We thank Peter Dixon, Timothy McNamara, and Chris Westbury for comments. This  
11 study is supported by a grant from NSERC to Weimin Mou.

12 Correspondence concerning this article should be addressed to Weimin Mou, Department  
13 of Psychology, P217 Biological Sciences Bldg, University of Alberta, Edmonton, Alberta,  
14 Canada, T6G 2E9. Email: [wmou@ualberta.ca](mailto:wmou@ualberta.ca).

15 The Matlab code of calculating position and heading estimates based on Mou & Zhang  
16 (2014) is placed at <https://doi.org/10.7939/R3FT8F06G>; the Matlab code based on (Friedman &  
17 Kohler, 2003) is placed at <https://doi.org/10.7939/r3-2tj7-xq22>. The Matlab code of simulation  
18 based on the self-localization hypothesis is placed at <https://doi.org/10.7939/R3QB9VM6J>.

19

20

1  
2  
3  
4  
5  
6  
7  
8  
9  
10  
11  
12  
13  
14  
15  
16  
17  
18  
19  
20  
21  
22

## Abstract

This study investigated when the Bayesian cue combination of piloting and path integration occurs in human homing behaviors. The Bayesian cue combination was hypothesized to occur in estimating the home location or self-localization. In Experiment 1, the participants learned the locations of five objects (one located at the learning position) in the presence of distal landmarks before walking a two-leg path without viewing the landmarks and objects. At the end of the path, the participants indicated the original locations of the objects in four cue conditions: 1) path integration only, 2) landmarks only where the participants were disoriented and the landmarks reappeared, 3) both path integration and the reappearing landmarks, and 4) path integration and conflicting landmarks rotated 45°. The participants' heading, position, and homing estimations were calculated. The ratio of the length of the second leg to that of the first leg was manipulated to be 0.5, 1, or 2. The results showed evidence of the Bayesian cue combination for heading estimates in all leg ratios, and for homing estimates in a small leg ratio (0.5) but not in a large leg ratio (2). The following experiments replicated the results of the Bayesian cue combination for heading but not for homing estimates for the large leg ratio (2) when participants did a typical homing task without learning the locations of objects (Experiment 2) and when proximal landmarks replaced distal landmarks (Experiments 3-4). These findings suggest that the Bayesian cue combination occurs in self-localization prior to homing.

Keywords: Bayesian cue combination, path integration, piloting, navigation, homing

## 1 **1. Introduction**

2           In navigation, humans update where they are located (i.e., position) and which direction  
3 they are facing (i.e., heading) relative to important items (e.g., home) in the environment. We  
4 refer to the process of updating the navigator's position and heading as self-localization. In  
5 general, navigation relies on two primary methods: *path integration* and *piloting* (Gallistel, 1990;  
6 Gallistel & Matzel, 2013; Mou & Wang, 2015; see Geva-Sagiv, Las, Yovel, & Ulanovsky, 2015  
7 for more specific categories). *Path integration* is a process by which people estimate their  
8 position and heading relying on self-motion cues (Etienne & Jeffery, 2004; Etienne et al., 1998;  
9 Loomis, Klatzky, Golledge, & Philbeck, 1999; Mittelstaedt & Mittelstaedt, 1980). *Piloting* is a  
10 process by which people estimate their position and heading relying on perceived landmarks  
11 (Etienne, Maurer, Boulens, Levy, & Rowe, 2004; Foo, Warren, Duchon, & Tarr, 2005; Wehner,  
12 Michel, & Antonsen, 1996). In addition to the different input cues (self-motion cues vs.  
13 perceived landmarks), path integration is continuous, whereas piloting is intermittent (Etienne &  
14 Jeffery, 2004; Wehner, Michel, & Antonsen, 1996; but see Tcheang, Bühlhoff, & Burgess, 2011).

15           *Homing*, going back to the origin of a path (i.e., home), is one of the most important  
16 navigation behaviors (e.g., Loomis et al., 1993). To understand human spatial navigation, several  
17 studies have examined the interaction between path integration and piloting in human homing  
18 behaviors (Chen, McNamara, Kelly, & Wolbers, 2017; Mou & Zhang, 2014; Nardini, Jones,  
19 Bedford, & Braddick, 2008; Sjolund, Kelly, & McNamara, 2018; Zhang & Mou, 2017, 2019;  
20 Zhao & Warren, 2015).

21           Some studies have investigated whether and how cue combinations of piloting and path  
22 integration occur to estimate home locations (Chen et al., 2017; Nardini et al., 2008; Sjolund et  
23 al., 2018; Zhao & Warren, 2015). In a typical paradigm, the participants start from the origin in

1 the presence of landmarks, and then walk a two-leg path with one turn. When they finish the  
2 outbound path, they walk back to the origin under the following different conditions. (1) In the  
3 *path integration only condition* (Path-Integration), the landmarks are removed before the  
4 participants walk back to the origin. (2) In the *landmark only condition* (Landmark), the  
5 participants are rotated for disorientation at the end of the outbound path and walk back to the  
6 origin in the presence of landmarks. (3) In the *both cues condition* (Both), the participants,  
7 without being disoriented, walk back to the origin in the presence of landmarks. (4) In the  
8 *conflicting cues condition* (Conflict), the participants, without being disoriented, walk back to the  
9 origin in the presence of the landmarks that have been rotated.

10 Using this paradigm, researchers examined the variance of observed homing errors in  
11 these four cue conditions and also the relative proximity of the mean observed homing errors to  
12 the predicted homing errors from path integration and from piloting (referred to as the observed  
13 weights) in the Conflict condition (e.g., Chen et al., 2017; Nardini et al., 2008; Sjolund et al.,  
14 2018; Zhao & Warren, 2015). In general, the majority of past studies found that human adults  
15 could optimally or suboptimally combine (i.e., in a Bayesian manner) the homing estimates from  
16 piloting and path integration (Chen et al., 2017; Nardini et al., 2008; Sjolund et al., 2018; but see  
17 Petrini, Caradonna, Foster, Burgess, & Nardini, 2016; Zhao & Warren, 2015).

18 Other studies have examined whether and how path integration and piloting interact in  
19 self-localization estimations prior to homing (Mou & Zhang, 2014; Zhang & Mou, 2017, 2019).  
20 Mou and Zhang (2014) showed that when the participants saw rotated distal landmarks after  
21 walking a path, their heading estimations were determined by the rotated landmarks, while their  
22 position estimations were still determined by path integration. Furthermore, Zhang and Mou  
23 (2017) reported that when the participants, after walking a path, saw a proximal visual landmark

1 that had been displaced to their testing position (at the end of the path), the participants' position  
2 estimations were determined by the displaced landmarks while their heading estimations were  
3 still determined by path integration. In Zhang and Mou (2019), the participants drove the  
4 outbound path in large-scale virtual environments. This study demonstrated both (A) displaced  
5 proximal landmarks reset participants' positions; (B) and rotated distal landmarks reset  
6 participants' headings. All these results showed that cue competition occurs in human heading or  
7 position estimations prior to homing estimations.

## 8 **1.2 Homing hypothesis and self-localization hypothesis**

9 It is theoretically important to determine the stages during which a cue combination  
10 occurs in human homing behaviors. We propose two hypotheses stipulating different stages  
11 (homing or self-localization) (see Figure 1). According to *the homing hypothesis*, the Bayesian  
12 cue combination only occurs in homing estimations.<sup>1</sup> Both path integration and piloting produce  
13 an independent homing estimate. These two homing estimates are then combined to form a final  
14 homing estimate. According to *the self-localization hypothesis*, the Bayesian cue combination  
15 occurs when determining the position and heading of the navigator (i.e., self-localization) prior  
16 to the homing estimation. Piloting and path integration do not produce two separate homing  
17 estimates. Instead, they produce separate position estimates and separate heading estimates that  
18 are then combined respectively. The combined position estimates and the combined heading  
19 estimates jointly determine the home location. We note that cue combination of self-localization  
20 estimates and cue combination of homing estimates both could occur either continuously or  
21 intermittently during the outbound path. We assume that path integration process occurs

---

<sup>1</sup> The previous studies in the literature only stated that home estimates are produced by path integration and piloting (e.g., Chen et al., 2017; Nardini et al., 2008), and did not explicitly state whether there are heading or position estimates in each process.

1 continuously and piloting occurs intermittently during the outbound path (e.g., Zhang & Mou,  
2 2017). Consequently, cue combination occurs intermittently regardless of the estimates to be  
3 combined (self-localization estimates or homing estimates)<sup>2</sup>.

4         These two hypotheses have different theoretical assumptions. The homing hypothesis  
5 implies that piloting and path integration are independent and use two different mental maps  
6 (Klatzky, 1998; Vickerstaff & Cheung, 2010). For example, while piloting uses an allocentric  
7 mental map consisting of spatial relations specified in terms of allocentric reference directions,  
8 path integration may use an egocentric mental map consisting of spatial relations specified in  
9 terms of egocentric reference directions (Benhamou, Sauvé, & Bovet, 1990; Fujita, Loomis,  
10 Klatzky, & Golledge, 1990; Wang & Spelke, 2002). Referring to the separate mental maps, path  
11 integration and piloting produce separate (independent) home location estimates. These two  
12 estimates are then combined to determine the home location.

13         In contrast, the self-localization hypothesis implies that piloting and path integration may  
14 not be completely independent and may use the same mental map rather than two different  
15 mental maps of locations in the environment (Gallistel & Matzel, 2013; Tcheang, Bühlhoff, &  
16 Burgess, 2011). Both piloting and path integration use the same mental map that specifies the  
17 spatial relations between locations in the environment (Zhang, Mou, & McNamara, 2011).  
18 Referring to the same mental map, people estimate their heading and position by combining the  
19 estimates from path integration and piloting, and then determine their home location using the  
20 estimated heading and position. Note that the current project does not specify or examine the  
21 exact form of spatial memories of locations. The form can be a single cognitive map (Tolman,

---

<sup>2</sup> We are grateful to one anonymous reviewer for this suggestion.

1 1948), a cognitive collage (Tversky, 1993), or a cognitive graph (Chrastil & Warren, 2014). We  
2 use the mental map to refer to all possible forms of spatial memories of locations.

3         The homing hypothesis is widely assumed by the studies examining cue combinations in  
4 human homing behaviors (e.g. Chen et al., 2017; Nardini et al., 2008; Sjolund et al., 2018).  
5 Moreover, the majority of studies have showed that homing errors for human adults in two-cue  
6 conditions (Both and Conflict conditions) can be predicted by the Bayesian cue combination of  
7 homing errors in single-cue conditions (Path-Integration and Landmark conditions). These  
8 findings are consistent with the homing hypothesis (Chen et al., 2017; Nardini et al., 2008;  
9 Sjolund et al., 2018; but see Zhao & Warren, 2015).

10         The literature also shows evidence of cue interactions in heading/position estimations  
11 prior to homing estimations in human studies (Mou & Zhang, 2014; Zhang & Mou, 2017, 2019),  
12 which is more consistent with the self-localization hypothesis than the homing hypothesis. In  
13 addition, in a path integration model for ants, Wehner, Michel, and Antonsen (1996; see also  
14 Freas, Narendra, & Cheng, 2017) proposed that ants used a skylight compass to determine their  
15 headings before calculating the homing vector, indicating that for ants, piloting cues (skylights)  
16 affect heading estimations in path integration. Etienne et al. (2004) showed that hamsters, after  
17 briefly seeing rotated environmental cues, went to the nest that was consistent with the rotated  
18 environmental cues, although these cues were not perceivable during homing. This finding  
19 indicates that the piloting cues (the rotated environmental cues) reset the heading/position  
20 estimations in path integration prior to homing. Neuroscience literature also shows that either  
21 path integration cues or landmarks can activate rodents' place cells or head direction cells  
22 (Muller, 1996; Taube, 2007). If we assume that rodents' place cells are responsible in  
23 representing rodents' positions and heading cells are responsible in representing rodents'

1 headings, path integration and piloting jointly determine position estimates and heading  
2 estimates for rodents similar to humans (e.g. Zhang & Mou, 2019).

3 As discussed above, the key difference between the homing hypothesis and the self-  
4 localization hypothesis is the claim of the stage in which the Bayesian cue combination occurs  
5 (in homing estimation or in self-localization estimation). Therefore, the most direct dissociation  
6 between these two hypotheses is to empirically investigate whether the Bayesian cue  
7 combination occurs in human self-localization estimates (i.e., heading and position estimates) or  
8 homing estimates. We acknowledge that it is also plausible that the Bayesian cue combination  
9 occurs in both self-localization estimates and homing estimates, incorporating the self-  
10 localization and the homing hypotheses. However, there is no study examining the Bayesian cue  
11 combination in homing and self-localization estimates simultaneously. Thus, at this point there is  
12 no empirical evidence that can directly dissociate the self-localization hypothesis from the  
13 homing hypothesis or incorporating these two hypotheses<sup>3</sup>.

### 14 **1.3 Current study**

15 The primary purpose of the current study was to distinguish between the homing  
16 hypothesis and the self-localization hypothesis by simultaneously examining the Bayesian cue  
17 combination of path integration and piloting in self-localization estimates and homing estimates.  
18 More evidence for the Bayesian cue combination in the self-localization estimates than in the  
19 homing estimates would favor the self-localization hypothesis. By contrast, more evidence for  
20 the Bayesian cue combination in the homing estimates than in the self-localization estimates  
21 would favor the homing hypothesis.

---

<sup>3</sup> We are grateful to one anonymous reviewer for this suggestion.

1           Following the previous studies (e.g., Nardini et al, 2008), we qualify the Bayesian cue  
 2 combination using two criteria: (1) variance reduction and (2) minimum variance in the two-cue  
 3 conditions. We will specify the testing equations of these two criteria below.

4           The Bayesian cue combination is the linearly weighted average of the estimates based on  
 5 each single cue, which leads to the minimum variance of the combined estimate among all  
 6 possible weights (Cheng, Shettleworth, Huttenlocher, & Rieser, 2007; Ernst & Banks, 2002).

7           A general linear weighted average is illustrated in the following equation:

$$8 \quad E_{12} = W_1 \times E_1 + W_2 \times E_2 \quad (1)$$

9           where  $E_{12}$  is the combined estimate in the presence of both cues, and  $E_1$  and  $E_2$  are the estimates  
 10 based on each single cue.  $W_1$  and  $W_2$  are the weights, ranging from 0 to 1, and  $W_1 + W_2 = 1$ .

11           Assuming that the estimates based on each single cue are independent, the variance of the  
 12 combined estimate can be calculated from the variances of each single cue:

$$13 \quad \sigma_{12}^2 = W_1^2 \times \sigma_1^2 + W_2^2 \times \sigma_2^2 \quad (2)$$

14           where  $\sigma_{12}^2$  is the variance of the combined estimate in the presence of both cues;  $\sigma_1^2$  and  $\sigma_2^2$  are  
 15 the variances of estimates based on each single cue.

16           Because the Bayesian combination leads to the minimum variance, it should produce a  
 17 variance reduction in the two-cue conditions (Both and Conflict conditions) compared with the  
 18 single-cue conditions (Path-Integration and Landmark conditions). However, it is not **always**  
 19 practical to test variance reductions in the two-cue conditions compared to both single-cue  
 20 conditions (i.e.  $\sigma_{12}^2 < \sigma_1^2$ , and  $\sigma_{12}^2 < \sigma_2^2$ ). When the estimation variability from one cue is much  
 21 smaller than that from the other cue, the estimation variability in the two-cue conditions may not

1 be significantly smaller than that in the more precise single-cue condition (Rohde, Van Dam, &  
 2 Ernst, 2016). In the most extreme case when one cue is valid but the other cue is not, the  
 3 Bayesian combination predicts that only the estimate of the valid cue contributes to the combined  
 4 estimate and the estimate from the invalid cue should be ignored. Therefore, in the current study,  
 5 we quantify variance reduction by an estimation variability in the two-cue conditions that is  
 6 significantly smaller than the less precise single-cue condition and no larger than the more  
 7 precise single-cue condition. In short, Equation 3 tests the criterion of variance reduction (see the  
 8 similar equation in Butler, Smith, Campos, & Bühlhoff, 2010, Equation 9). We will discuss the  
 9 implications of using this testing equation in the General Discussion.

$$10 \quad \sigma_{12}^2 \leq \min(\sigma_1^2, \sigma_2^2) \quad (3)$$

11 More strictly, in the Bayesian combination, the weight assigned to each cue is inversely  
 12 proportional to the estimation variance based on the cue. The weight leading to the minimum  
 13 variance (*optimal variance*) is termed *the optimal weight*. The following equations illustrate how  
 14 to calculate the optimal weight and variance from the variance of the estimate based on each  
 15 single cue. These two equations together test the criterion of minimum variance. In the extreme  
 16 case when one cue is valid but the other cue is not, the variance of one cue is way larger than that  
 17 of the other. Suppose  $\sigma_2^2 \gg \sigma_1^2$ , thus  $W_{1_{optimal}} = 1$  and  $\sigma_{12_{optimal}}^2 = \sigma_1^2$ .

$$18 \quad W_{1_{optimal}} = \frac{\sigma_2^2}{\sigma_1^2 + \sigma_2^2}, \quad \sigma_{12_{optimal}}^2 = \frac{\sigma_1^2 \times \sigma_2^2}{\sigma_1^2 + \sigma_2^2} \quad (4)$$

### 19 **1.3.1 General methods**

20 The current study used the same four cue conditions (Path-Integration, Landmark, Both,  
 21 and Conflict) as in previous studies (Chen et al., 2017; Nardini et al., 2008; Sjolund et al., 2018;  
 22 Zhao & Warren, 2015). In an immersive virtual environment, participants walked two-leg paths

1 with the presence of landmarks. After walking, participants indicated the home location in the  
2 conditions of Path-Integration, Landmark, Both, and Conflict. In the Conflict condition, the  
3 landmarks were rotated around the testing position (i.e., the end of the second leg).

4         There are two more characteristics in the methods of the current study. First, following  
5 Mou and Zhang (2014), the current study asked participants to remember the locations of five  
6 objects (one at the origin) and then indicate the original locations of these objects after  
7 navigation in order to simultaneously measure heading error, position error, and homing error.  
8 Second, the current study manipulated the leg ratio of the second leg (L2) to the first leg (L1) of  
9 a path (L2/L1). These two characteristics were inspired by a mathematical model elaborating on  
10 the self-localization hypothesis.

11         The first premise of this model states that the heading error ( $\eta$ ) and the position angular  
12 error ( $\pi$ ) jointly determine the homing angular error ( $\theta$ ) according to the following equation.  
13 Explanations and derivations of this equation are shown in Figure 2 (see also Mou & Zhang,  
14 2014; Zhang & Mou, 2017, 2019).

$$15 \quad \theta = \pi - \eta \quad (5)$$

16         In a typical homing paradigm, participants only reported the home location, producing  
17 only the measure of  $\theta$  (Chen et al., 2017; Nardini et al., 2008; Sjolund et al., 2018; Zhao &  
18 Warren, 2015). According to Equation 5, we cannot determine two unknown errors (i.e.,  $\pi$  and  $\eta$ )  
19 from one measured error (i.e.,  $\theta$ ). To calculate the position and heading errors in addition to the  
20 homing error, Mou and Zhang (2014) developed a method to calculate the position and heading  
21 errors from the replaced locations of five objects (see Mou & Zhang, 2014; Zhang and Mou,  
22 2017 for the method details; see the Matlab code implementing this method at

1 <https://doi.org/10.7939/R3FT8F06G>). However, the method of Mou and Zhang (2014) only  
 2 measured the angular errors but did not measure two-dimensional locational errors. A two-  
 3 dimensional locational error is comprised of both angular and length errors. Thus, the current  
 4 study did not use the method of Mou and Zhang (2014).

5         Instead, the current study used bidimensional regression (Friedman & Kohler, 2003) to  
 6 calculate participants' estimated positions ( $P'$ ) and headings ( $h'$ )<sup>4</sup>. Figure 3 illustrates the general  
 7 ideas used to implement the bidimensional regression (see the Matlab code online  
 8 <https://doi.org/10.7939/r3-2tj7-xq22>). Briefly, the bidimensional regression technique established  
 9 a regression model to predict the original locations of objects (e.g.,  $O$ , a dependent variable)  
 10 from the replaced locations of objects (e.g.,  $O'$ , an independent variable). The regression model  
 11 can be described as  $O \approx f(O')$ .  $f$  is the prediction function. We assume that the relationship  
 12 between the replaced locations of objects ( $O'$ ) and the testing position/heading ( $P/h$ ) is similar to  
 13 the relationship between the original locations of objects ( $O$ ) and the estimated position/heading  
 14 ( $P'/h'$ ). Hence, the regression model also predicted the estimated position and heading from each  
 15 participant's testing position and heading respectively, i.e.  $P' = f(P)$ ,  $h' = f(h)$ .

16         The second premise of the mathematical model states that in path integration, the position  
 17 angular error ( $\pi_{PI}$ ) depends on the heading error ( $\eta_{PI}$ ) (see Figure 4). This is because the position  
 18 angular error ( $\pi_{PI}$ ) depends on the error made when estimating the turning angle between the  
 19 first and second legs in the outbound path (i.e., the walking direction of the second leg, see Fujita  
 20 et al., 1993), and the heading error ( $\eta_{PI}$ ) measures the error made when estimating the turning  
 21 angle. Furthermore, the position angular error's dependence on the heading error increases with

---

<sup>4</sup> The bidimensional regression method yielded the same results as the method of Mou and Zhang (2014) in terms of the angular errors only.

1 the path's leg ratio (L2/L1) Three examples in Figure 4 illustrate this idea. Generalizing from  
 2 these examples, we assume that the position error ( $\pi_{PI}$ ) and the heading error both from path  
 3 integration ( $\eta_{PI}$ ) follow a linear relationship<sup>5</sup>:

$$4 \quad \pi_{PI} = a \times \eta_{PI} \quad (6)$$

5  $a$  is the slope of the linear relationship. Slope  $a$  is assumed to increase with the leg ratio  
 6 (e.g.,  $a$  is 0, 0.5, and 1 for the leg ratio of 0, 1, and  $\infty$ , respectively).

7 Based on these two premises, the mathematical model can be fully developed (see the full  
 8 details of the mathematical model in Appendix 1). This model predicts that variance reduction  
 9 occurs in heading estimates but not in homing estimates when the leg ratio is large. Here, we  
 10 illustrate this prediction using one example (see the detailed explanations and derivations in  
 11 Appendix 2).

12 This example has experimental procedures similar to those in previous studies (e.g.,  
 13 Nardini et al, 2008), except for one modification. Different from the previous study, distal  
 14 landmarks are placed far from participants such that landmarks do not indicate participants'  
 15 positions. Hence, the distal landmarks do not contribute to the position errors. As in the previous  
 16 studies, the participants walk towards the testing position in all four cue conditions. Therefore,  
 17 they use path integration to update their position representations in the outbound path before  
 18 ending at the testing position in all cue conditions. Moreover, in the Landmark condition, the

---

<sup>5</sup> According to trigonometry, the position angular error ( $\pi_{PI}$ ) and the heading error both from path integration ( $\eta_{PI}$ ) do not necessarily follow a linear relationship for all leg ratios although the linear relationships hold in these three examples. We use a linear relationship for the sake of simplicity of modelling, assuming it is valid for human path integration regardless of the leg ratio (see Maurer & Séguinot, 1995).

1 participants are disoriented in place at the testing position. Consequently, after disorientation, the  
 2 position estimate from path integration is intact although the heading estimate from path  
 3 integration is disrupted (Mou & Zhang, 2014). Hence, the position error in the Landmark, Both,  
 4 and Conflict conditions is the same as that in the Path-Integration condition (i.e.,  $\pi_{Both} = \pi_{PI}$ ,  
 5  $\pi_{LM} = \pi_{PI}, \pi_{Conflict} = \pi_{PI}$ ).

6 As shown in Figure 4, when the leg ratio (L2/L1) is large, the position angular error from  
 7 path integration ( $\pi_{PI}$ ) is highly dependent on the heading error from path integration ( $\eta_{PI}$ ). To  
 8 reflect this high dependence, suppose  $\pi_{PI} = 0.7 \times \eta_{PI}$ . We also suppose that the variance of  
 9 heading estimates is significantly smaller in the Landmark condition than in the Path-Integration  
 10 condition (e.g., Zhao & Warren, 2015). To reflect the variance, suppose  $\sigma_{\eta_{LM}}^2 = 0.25 \times \sigma_{\eta_{PI}}^2$ .  
 11 According to the self-localization hypothesis, the Bayesian combination occurs in the heading  
 12 estimates. Thus,  $W_{LM} = 4 \times W_{PI}$  (see Equation 4). As a result,  $\eta_{Both} = 0.2 \times \eta_{PI} + 0.8 \times$   
 13  $\eta_{LM}$ . According to Equation 5 (i.e.,  $\theta = \pi - \eta$ ),  $\theta_{PI} = \pi_{PI} - \eta_{PI} = 0.7 \times \eta_{PI} - \eta_{PI} = -0.3 \times$   
 14  $\eta_{PI}$ . Thus,  $\sigma_{\theta_{PI}}^2 = 0.09 \times \sigma_{\eta_{PI}}^2$ . This example suggests that  $\sigma_{\theta_{PI}}^2$  can be very small when  $\pi_{PI}$   
 15 highly depends on  $\eta_{PI}$  (i.e., when the leg ratio is large). Conceptually, it occurs because  $\pi_{PI}$  and  
 16  $\eta_{PI}$  share a large error ( $0.7 \times \eta_{PI}$ ) and this shared error is cancelled out in calculating  $\theta_{PI}$ . Maurer  
 17 and Séguinot (1995, Figure 8) reported that the homing angular error ( $\theta_{PI}$ ) linearly decreases  
 18 with the increase of the segment ratio (L2/L1) in the homing behaviors of mammals without  
 19 vision.

20 In contrast,  $\theta_{Both} = \pi_{Both} - \eta_{Both} = \pi_{PI} - \eta_{Both} = 0.7 \times \eta_{PI} - (0.2 \times \eta_{PI} + 0.8 \times$   
 21  $\eta_{LM}) = 0.5 \times \eta_{PI} - 0.8 \times \eta_{LM}$ . Note that  $\eta_{PI}$  and  $\eta_{LM}$  are independent.  $\sigma_{\theta_{Both}}^2 = 0.25 \times$   
 22  $\sigma_{\eta_{PI}}^2 + 0.64 \times \sigma_{\eta_{LM}}^2$ . As assumed above,  $\sigma_{\eta_{LM}}^2 = 0.25 \times \sigma_{\eta_{PI}}^2$ . Thus,  $\sigma_{\theta_{Both}}^2 = 0.25 \times$

1  $\sigma_{\eta_{PI}}^2 + 0.16 \times \sigma_{\eta_{PI}}^2 = 0.41 \times \sigma_{\eta_{PI}}^2$ . We get  $\sigma_{\theta_{Both}}^2 > \sigma_{\theta_{PI}}^2$ . Conceptually, due to the  
 2 combination in heading estimation ( $\eta_{Both} = 0.2 \times \eta_{PI} + 0.8 \times \eta_{LM}$ ) and the independence  
 3 between  $\eta_{PI}$  and  $\eta_{LM}$ , only a small proportion (i.e.,  $0.2 \times \eta_{PI}$ ) of contributions of  $\pi_{Both}$  and  $\eta_{Both}$   
 4 to  $\theta_{Both}$  can be cancelled out.

5 In this example, when the leg ratio (L2/L1) is large, we get  $\sigma_{\theta_{Both}}^2 > \sigma_{\theta_{PI}}^2$ , indicating no  
 6 variance reduction (i.e.,  $\sigma_{12}^2 > \min(\sigma_1^2, \sigma_2^2)$ , meaning no Bayesian combination) in homing  
 7 estimates.

8 When the leg ratio (L2/L1) is small, as discussed above, there is a low dependency  
 9 between  $\pi_{PI}$  and  $\eta_{PI}$ . To reflect that low dependency, suppose  $\pi_{PI} = 0.3 \times \eta_{PI}$ . Then,  $\theta_{PI} =$   
 10  $\pi_{PI} - \eta_{PI} = 0.3 \times \eta_{PI} - \eta_{PI} = -0.7 \times \eta_{PI}$ . As a result,  $\sigma_{\theta_{PI}}^2 = 0.49 \times \sigma_{\eta_{PI}}^2$ . In contrast,  
 11  $\theta_{Both} = \pi_{Both} - \eta_{Both} = \pi_{PI} - \eta_{Both} = 0.3 \times \eta_{PI} - (0.2 \times \eta_{PI} + 0.8 \times \eta_{LM}) = 0.1 \times$   
 12  $\eta_{PI} - 0.8 \times \eta_{LM}$ . Thus  $\sigma_{\theta_{Both}}^2 = 0.01 \times \sigma_{\eta_{PI}}^2 + 0.64 \times \sigma_{\eta_{LM}}^2$ . Note that  $\sigma_{\eta_{LM}}^2 = 0.25 \times \sigma_{\eta_{PI}}^2$ .  
 13 Consequently,  $\sigma_{\theta_{Both}}^2 = 0.01 \times \sigma_{\eta_{PI}}^2 + 0.16 \times \sigma_{\eta_{PI}}^2 = 0.17 \times \sigma_{\eta_{PI}}^2$ . We get  $\sigma_{\theta_{Both}}^2 < \sigma_{\theta_{PI}}^2$ . In  
 14 addition,  $\theta_{LM} = \pi_{LM} - \eta_{LM} = \pi_{PI} - \eta_{LM} = 0.3 \times \eta_{PI} - \eta_{LM}$ . Thus,  $\sigma_{\theta_{LM}}^2 = 0.09 \times \sigma_{\eta_{PI}}^2 +$   
 15  $\sigma_{\eta_{LM}}^2$ . As a result,  $\sigma_{\theta_{LM}}^2 = 0.09 \times \sigma_{\eta_{PI}}^2 + 0.25 \times \sigma_{\eta_{PI}}^2 = 0.34 \times \sigma_{\eta_{PI}}^2$ . We get  $\sigma_{\theta_{Both}}^2 <$   
 16  $\sigma_{\theta_{LM}}^2$  as well. As  $\sigma_{\theta_{Both}}^2 < \sigma_{\theta_{PI}}^2$  and  $\sigma_{\theta_{Both}}^2 < \sigma_{\theta_{LM}}^2$ , this indicates a variance reduction (i.e.,  
 17  $\sigma_{12}^2 \leq \min(\sigma_1^2, \sigma_2^2)$ , a signature of the Bayesian cue combination) in homing estimates.

18 A simulation based on this mathematical model in Appendix 2 also demonstrates that  
 19 when the leg ratio (L2/L1) is large, the Bayesian combination in heading estimates likely leads to  
 20 no variance reduction in homing estimates whereas when the leg ratio is small, the Bayesian  
 21 combination in heading estimates likely leads to reduced variances in homing estimates.  
 22 Therefore, in the current study, we manipulated the leg ratio to dissociate the self-localization

1 hypothesis from the homing hypothesis. The self-localization hypothesis predicts that heading  
2 estimates follow the Bayesian combination in all leg ratios. The homing estimates will not follow  
3 the Bayesian combination, especially for a large leg ratio. In contrast, the homing hypothesis  
4 predicts that homing estimates follow the Bayesian combination in all leg ratios. However, it  
5 does not predict the Bayesian cue combination for heading estimates in any leg ratio. As the first  
6 attempt to dissociate the self-localization hypothesis from the homing hypothesis, to easily  
7 contrast the homing and the self-localization hypotheses, the current study systematically  
8 examined the Bayesian cue combination in heading and homing estimates but not in position  
9 estimates.

## 10 **2. Experiment 1**

11 Following the example discussed above, Experiment 1 dissociated the self-localization  
12 hypothesis from the homing hypothesis by manipulating the leg ratio. The participants learned  
13 the locations of five objects in the presence of the distal landmarks at the path origin (O in Figure  
14 5A) in an immersive virtual reality environment. The participants then physically walked two-leg  
15 paths (O-T-P) after the objects and the distal landmarks were removed. After walking each path,  
16 the participants indicated the original locations of the five objects in the four cue conditions.  
17 Importantly, three groups of participants had different leg ratios of the second leg over the first  
18 leg (i.e.,  $L2/L1 = 0.5, 1, \text{ and } 2$ ). We examined whether Bayesian cue combination occurred in  
19 heading or homing estimates in different leg ratio groups. The Bayesian cue combination for  
20 heading estimates in all leg ratios and no Bayesian cue combination for homing estimates in the  
21 large leg ratio would support the self-localization hypothesis. By contrast, the Bayesian cue  
22 combination for homing estimates in all leg ratios and no Bayesian cue combination for heading  
23 estimates in any leg ratio would support the homing hypothesis.

## 1 2.1 Method

### 2 2.1.1 Participants

3 Eighty-four university students<sup>6</sup> (42 men and 42 women) participated in the experiment  
4 (28 for each leg ratio group with 14 men and 14 women) to fulfill a partial requirement for an  
5 introductory psychology course. Before the experiment, all participants signed the consent form  
6 approved by the University of Alberta Research Ethics Board.

7 In Nardini et al. (2008), Cohen's *ds* indicating variance reduction in the Both condition  
8 compared with single-cue conditions were 0.92 (Both vs. Landmark) and 2.33 (Both vs. Path-  
9 Integration).<sup>7</sup> Assuming Cohen's  $d = 0.92$ , we used 28 participants for each leg ratio group to get  
10 a power value of 0.91 at the 0.05 level (for two-tailed paired *t* test) to detect the variance  
11 reduction in the Both condition.

### 12 2.1.2 Materials and Design

13 The experiment was conducted in a 4-by-4m physical room. A virtual environment  
14 containing a grass-textured field and a distal circular wall was rendered using the Worldviz  
15 Vizard (<http://www.worldviz.com/>, Santa Barbara, California). The virtual environment was  
16 displayed in stereo with an nVisor SX60 head-mounted display (HMD) (NVIS, Inc. Virginia).  
17 The HMD had dual SXGA microdisplays with 1280x1024 24-bit color pixels per eye and a 60°  
18 diagonal field-of-view. The refresh rate was 60Hz. The head motion of participants was tracked  
19 with an InterSense IS-900 motion tracking system (InterSense, Inc., Massachusetts). The  
20 sampling rate was 180Hz and the resolution was 0.75mm and 0.05°.

---

<sup>6</sup> About 20% participants dropped out due to motion sickness and were replaced.

<sup>7</sup> Cohen's *d* was calculated by  $t\sqrt{\frac{2}{N}}$ . In Nardini et al. (2008), the *t* value was 6.8 for the contrast between Both and Path-Integration and 2.7 for the contrast between Both and Landmark. *N* was 17.

1           Three shapes (a circle, rectangle, and polygon) on a circular wall with a radius of 50m  
2 and a height of 10m served as distal landmarks (Figures 5A and 5B). A virtual blue stick was  
3 connected to an InterSense IS-900 wand for pointing. Similar to moving a cursor by controlling a  
4 mouse on the computer screen, the participants could move the wand to control the movement of  
5 the virtual stick to point to positions in the virtual environment.

6           For each path, the origin (O) and the turning point (T) were indicated by two red poles,  
7 and the testing position (P) was indicated by a green pole. All poles were 2m in height, and  
8 0.05m in radius. The poles were presented in sequence to guide the participants' walking (Zhao  
9 & Warren, 2015). The poles disappeared once the participants arrived at their positions.

10           The object configuration, which participants learned at O (Figure 5A) and rebuilt after  
11 they had walked a path (while standing at the testing position P and adopting the testing heading  
12  $h$ , Figure 5B), included five objects (a ball, brush, clock, mug, and phone). One object was  
13 located at the origin (O in Figure 5C). The other four objects (X1 to X4 in Figure 5C) were  
14 located 1.41m from O in the directions of 45°, 135°, 225°, and 315° clockwise from the direction  
15 of the first leg. The associations between objects and positions were random across participants  
16 but were consistent across trials for each participant.

17           There were three leg ratios for paths ( $L2/L1 = 2, 1, \text{ and } 0.5$ ). For  $L2/L1 = 2$  (Figure 5D),  
18 the 1<sup>st</sup> leg was 0.9m and the 2<sup>nd</sup> leg was 1.8m. For  $L2/L1 = 1$ , both legs were 1.8m (Figure 5E).  
19 For  $L2/L1 = 0.5$ , the 1<sup>st</sup> leg was 1.8m and the 2<sup>nd</sup> leg was 0.9m (Figure 5F). The turning angle  
20 could be 50° or 130° clockwise or counter-clockwise, forming four paths for each leg ratio.

21           The shapes on the wall (i.e., the distal landmarks) were removed when the participants  
22 reached the turning point (T), although the bare wall remained. Whether and how the shapes

1 reappeared depended on the cue condition. The four cue conditions differed only after  
2 participants reached the testing position (P). In the Path-Integration condition, the participants  
3 only undertook a counting task (repeatedly subtracting three from a starting number) for eight  
4 seconds. In the Landmark condition, the participants were rotated in a spinning chair ( $\sim 90^\circ$  per  
5 second) while counting. After the counting task, the shapes on the wall reappeared. In the Both  
6 condition, the shapes reappeared after the counting task.

7           The Conflict condition was the same as the Both condition, except that the shapes  
8 reappeared at  $45^\circ$  clockwise or counter-clockwise from the original direction (the counter-  
9 clockwise rotation is shown in Figure 5B). The rotation direction of the shapes was the same for  
10 each participant, while it was clockwise for half of the participants. As we wanted to examine the  
11 Bayesian cue combination of path integration and piloting whether in self-localization or  
12 homing, we shifted landmarks  $45^\circ$  in the Conflict condition. We speculated that a  $45^\circ$  conflicting  
13 direction was not too large to see the Bayesian cue combination whether it occurs in homing or  
14 heading/position estimations. It is believed that the Bayesian cue combination occurs when  
15 landmarks are slightly or moderately shifted, whereas cue competition occurs when the  
16 predictions from the two cues differ significantly (Körding et al., 2007; Sjolund et al., 2018;  
17 Zhao & Warren, 2015). Meanwhile,  $45^\circ$  was not too small of a shift to detect a weighted average  
18 in cue combination. If the shift angle was too small, then the experiment might not be able to  
19 detect the difference of a weighted average from either of the predictions based on landmarks  
20 and path integration.

21           Twenty-eight participants (14 men and 14 women) were randomly assigned to each of the  
22 three leg-ratio groups ( $L2/L1 = 0.5, 1, \text{ or } 2$ ). All participants completed the four paths for their

1 group in each of the four cue conditions (16 trials in total). For each participant, the 16 trials  
2 were randomly ordered. For each trial, the five indicated locations were recorded.

### 3 **2.1.3 Procedure**

4 For each experimental trial, there was a learning phase and a testing phase. The  
5 participants first looked for a red pole that was placed in the origin (O) in the grass-textured field  
6 and walked towards it. Once they reached the pole, it disappeared, and the second red pole that  
7 was placed in the turning point (T) appeared. The participants were instructed to turn to face the  
8 second pole to adopt their learning orientation, which was the same as the first walking leg. After  
9 the participants faced the second red pole, it disappeared.

10 The learning phase then started. The wall with the shapes and five objects appeared. The  
11 participants learned the directions of the shapes and the locations of the objects (for three  
12 minutes in the first trial and 30 seconds in the remaining 15 trials, as the landmarks and objects  
13 remained at the same locations in all trials). During learning, participants stayed at the learning  
14 location (O) and retained their learning orientation (facing the first walking leg, the direction  
15 from O to T) although they were allowed to view the landmarks and objects over their shoulder if  
16 necessary.

17 Afterwards, the landmarks and objects were removed. The participants were asked to use  
18 the wand to indicated the locations of the five objects and the directions of the three landmarks,  
19 probed by a small model of each at the bottom left corner of the HMD in a random order, by  
20 pointing the virtual stick toward the remembered locations of the objects or directions of the  
21 shapes. Feedback was given by presenting the probed object or shape at the correct location for  
22 five seconds. The participants had two rounds of such replacing and feedback (for all 16 trials to  
23 make sure they had an accurate memory of the objects' locations at each trial).

1           After the learning phase, the objects disappeared and the participants started to walk the  
2 path. A red pole appeared at the turning position (T in Figures 5D, 5E, and 5F) and guided the  
3 participants to walk towards it. Once the participants reached the pole, the shapes on the wall  
4 (i.e., the landmarks) as well as the pole disappeared. A green pole at the testing position  
5 (illustrated as P in Figures 5D, 5E, and 5F) appeared and guided the participants to walk towards  
6 it. Once they reached it, it disappeared. The procedure so far was the same for all cue conditions  
7 and differed afterwards. In the Path-Integration, Both, and Conflict conditions, the participants  
8 completed the counting task for eight seconds while they stood at P. In the Landmark condition,  
9 the participants sat in a swivel chair and were rotated for 8s while they were completing the  
10 counting task. In the Landmark, Both, and Conflict conditions, the shapes reappeared after the  
11 eight seconds. For all cue conditions, the participants indicated the locations of all five objects,  
12 probed in a random order, using the wand. No feedback was given. Participants were allowed to  
13 turn their bodies while indicating the original locations of the objects.

14           After the participants indicated the locations of all objects, all visual items in the virtual  
15 environment except the grass-textured field disappeared and the participants were led to a  
16 random location in the physical room. A red pole was placed at the origin of the next path to start  
17 the next trial.

18           Before the experimental trials, to familiarize themselves with the procedure, the  
19 participants did a practice trial with different objects and a different path.

## 20 **2.1.4 Data Analysis**

### 21 ***2.1.4.1 Measuring estimates of position and heading***

22           We used the bidimensional regression (Friedman & Kolner, 2003) to model the  
23 relationship between the correct locations (dependent variable) and replaced locations

1 (independent variable) of the five objects for each trial (i.e., path) (Figure 3). The preliminary  
 2 analyses of the data showed that the mean  $r^2$  for the regression models across paths and  
 3 participants was larger than .80 in the experiments conducted for the current study. This indicates  
 4 a very high coherence in responses across objects within individual paths. More important, it  
 5 confirmed our assumption that the participants used the remembered original locations of objects  
 6 (e.g., O, X1 to X4) from the estimated position ( $P'$ ) and heading ( $h'$ ) to guide their responses of  
 7 replacing objects (e.g., O', X1' to X4') from their testing position (P) and heading ( $h$ ).  
 8 Consequently, the prediction function ( $f$ ) of the bidimensional regression model for each trial was  
 9 used to calculate the estimated position ( $P'$ ) and heading ( $h'$ ) using the participants' testing  
 10 position (P) and heading ( $h$ ) as the independent values respectively ( $P' = f(P)$ ,  $h' = f(h)$ ).

#### 11 ***2.1.4.2 Measuring estimation errors including angular, distance, and length errors***

12 We calculated the angular error for all heading, position, and homing estimates ( $\eta$ ,  $\pi$ ,  $\theta$ ,  
 13 see Figure 2). For the position and homing estimates, we calculated the two-dimensional distance  
 14 errors (the distance differences between the estimated and correct locations in both x and y  
 15 coordinates). We also calculated the length error (the difference between the correct and  
 16 estimated lengths, i.e.,  $\|\overrightarrow{PO'}\| - \|\overrightarrow{PO}\|$  for homing length errors,  $\|\overrightarrow{OP'}\| - \|\overrightarrow{OP}\|$  for position length  
 17 errors). Specifically, for the homing estimates, we transformed the coordinate system (using  
 18 rotation, translation, and uniform scale) such that the original home location O was (0, 0) and the  
 19 testing position P was (0, -1) in the new coordinate system. Hence, each individual homing two-  
 20 dimensional distance error was represented by the coordinate (x, y) of the replaced location of  
 21 the home location, i.e. O', in the new coordinate system for different paths and different cue  
 22 conditions in the standardized way. The length error was represented by the distance from P to O'

1 subtracting that from P to O (i.e.,  $\|\overrightarrow{PO'}\| - 1$ ). Similarly, for the position estimates, we transformed  
 2 the coordinate system such that P was (0, 0) and O was (0, -1).

3 In the Conflict condition, we flipped the sign of the individual angular error (i.e., heading  
 4 error, position error, and homing error) for the participants who experienced the clockwise  
 5 rotation of the landmarks. Therefore, the predicted heading error ( $\eta$ ) indicated by the rotated  
 6 distal landmarks (all rotated  $-45^\circ$  now) would be  $45^\circ$ . The homing angular error ( $\theta$ ) indicated by  
 7 the rotated distal landmarks would be  $-45^\circ$ . For the distance errors of homing estimates, as the  
 8 landmarks were rotated around the testing position P (0, -1) in the new coordinate system, we  
 9 changed (x, y) to (-x, y). Hence, for all participants, the predicted home location indicated by the  
 10 rotated distal landmarks would be  $(\sin(-45), \cos(-45) - 1)$ . Note that the rotation of the  
 11 landmark around the testing position should not have any effect on the length error.

12 We then calculated each participant's estimation bias in the Conflict condition for angular  
 13 and distance errors and estimation variability in each cue condition for angular, distance, and  
 14 length errors.

15 For angular errors, each participant's estimation bias was the circular mean of errors  
 16 across paths. The estimation variability was the circular standard deviation (SD) of errors across  
 17 paths. We used the following equation to calculate the observed weight assigned to the landmark  
 18 cue (the observed landmark weight,  $W_{ELM-observed}$ ) in heading or homing estimations in the  
 19 Conflict condition for each participant<sup>8</sup>. The estimate predicted by the landmark

---

<sup>8</sup> Due to noise, the observed means of errors of individual participants may lie outside the range of the predictions. Accordingly, we allowed the observed weight for each participant to be larger than one or smaller than zero. However, the mean observed weights for all groups were confirmed to be in the range of 0 and 1.

1 cue,  $E_{LM-predict}$ , was  $45^\circ$  for heading errors and  $-45^\circ$  for homing errors. The estimate predicted  
 2 by path integration,  $E_{PI-predict}$ , was  $0^\circ$ .  $E_{Conflict-observed}$  was the observed estimate in the  
 3 Conflict condition.

$$4 \quad W_{E_{LM-observed}} = \frac{E_{Conflict-observed} - E_{PI-predict}}{E_{LM-predict} - E_{PI-predict}} \frac{E_{Conflict-observed}}{E_{LM-predict}} \quad (7)$$

5 For two-dimensional distance errors, each participant's estimation bias was the signed  
 6 means estimates across paths  $(\bar{x}, \bar{y})$ . This bias was used to calculate the relative proximity in the  
 7 Conflict condition as did in the previous studies (e.g. Nardini et al., 2008). Estimation variability  
 8 was the square root of the mean squared distance from individual estimates  $(x, y)$  to  $(\bar{x}, \bar{y})$ , the  
 9 same as  $\sqrt{\sigma_x^2 + \sigma_y^2}$ . For length errors, estimation variability was the SD of errors across paths.

10 Preliminary analyses showed that participants tended to overshoot the distances between  
 11 the objects and their testing positions. This occurred because the length of the virtual stick used  
 12 to indicate the locations of the objects might have been underestimated in the virtual  
 13 environments (Mou & Zhang, 2014, p. 556). As a result, each response home,  $O'$   $(x, y)$ , within  
 14 each cue condition was moved towards or outwards from  $P(0, -1)$  with the same scale factor so  
 15 that the average length of  $\overline{PO'}$  across different paths within each cue condition was one (the same  
 16 as the correct length in the transformed coordinate). This adjustment did not change the direction  
 17 of  $\overline{PO'}$ . The adjusted  $O'$   $(x, y)$  was then used to calculate the estimation variability for distance  
 18 errors and length errors. The adjusted  $O'$   $(x, y)$  in the Conflict condition was also used to  
 19 calculate the relative proximity of observed  $O'$  to the original  $O(0, 0)$  and to the displaced  $O$   
 20  $(\sin(-45), \cos(-45) - 1)$  predicted by the rotated landmark. This relative proximity measured  
 21 the cue weights for two-dimensional distance errors.

1           The participants' estimation bias in the Conflict condition (indicating cue weights) and  
2 estimation variability in each cue condition were then used for the Bayesian cue combination  
3 analyses.

4           We examined the Bayesian cue combination primarily for heading and homing errors.  
5 The Bayesian cue combination analyses for position errors are not meaningful because in all cue  
6 conditions, the position error was only from path integration ( $\pi_{Both} = \pi_{PI}$ ,  $\pi_{LM} = \pi_{PI}$ ,  
7  $\pi_{Conflict} = \pi_{PI}$ ). The observed SDs of position estimates should be the same across all cue  
8 conditions. Therefore, no Bayesian cue combination for position estimations was expected. We  
9 present the SDs of position estimates only to check if they were the same across the cue  
10 conditions.

## 11 **2.2 Results**

12           In this and all following experiments, the length errors for position and homing estimates  
13 were the same across all cue conditions, thus not useful to test the Bayesian cue combination.  
14 The results of the two-dimensional distance errors were generally similar to the results of the  
15 angular errors for position and homing estimates (see the details in the supplementary materials  
16 and Table S1). In addition, there were only angular errors for heading estimates. In the interest of  
17 brevity, we only present the cue combination analyses for the angular errors. The results of the  
18 two dimensional distance errors and length errors are presented in the supplementary materials.

### 19 **2.2.1 Homing angular errors**

20           The circular means of the homing angular errors (Table 1) showed clear biases for the  
21 Conflict conditions in all of the leg ratio groups. According to the 95% confidence interval, the  
22 circular means significantly differed from 0°.

1           The SDs of homing angular errors were analyzed using mixed-model ANOVAs, with a  
 2 within-participant variable of the cue condition and a between-participant variable of the leg  
 3 ratio. Figure 6 plots the mean SDs of homing errors for the four cue conditions and the three  
 4 different leg ratios. Mean optimal SDs are also plotted.

5           The main effect of the cue condition was significant,  $F(3, 243) = 3.89, p = .01$ .  $MSE =$   
 6  $292.83, \eta_p^2 = .05$ . The main effect of the ratio was not significant,  $F(1, 81) = 1.89, p = .16$ .  $MSE$   
 7  $= 843.93, \eta_p^2 = .05$ . The interaction between the cue condition and leg ratio was significant,  $F(6,$   
 8  $243) = 4.46, p < .001$ .  $MSE = 292.83, \eta_p^2 = .10$ .

9           Because there was an interaction between the cue condition and leg ratio, repeated  
 10 measures ANOVAs were used to analyze the cue effect for each leg ratio group.

11           **For the group of L2/L1=2**, the main effect of the cue condition was significant,  $F(3, 81)$   
 12  $= 4.51, p < .01$ .  $MSE = 272.44, \eta_p^2 = .14$ . Planned contrasts showed that the mean SD in the Both  
 13 condition was significantly larger than that in the Path-Integration condition,  $t(27) = 2.40, p$   
 14  $= .02$ , Cohen's  $d = 0.64$ . The mean SD in the Both condition was not significantly different from  
 15 that in the Landmark condition,  $t(27) = 0.31, p = .76$ , Cohen's  $d = 0.08$ . For this and all null  
 16 effects of comparisons below, we calculated the Bayesian Factor ( $BF_{01}$ ) favoring the null effect  
 17 over the alternative. If the  $BF_{01}$  was larger than 3, then it favored the null effect. If the  $BF_{01}$  was  
 18 smaller than 1/3, then it favored the alternative (Rouder et al., 2009). The  $BF_{01}$  for this null effect  
 19 was 6.53. The mean SD in the Conflict condition was significantly larger than that in the Path-  
 20 Integration condition,  $t(27) = 3.60, p < .01$ , Cohen's  $d = 0.96$ . The mean SD in the Conflict  
 21 condition was not significantly different from that in the Landmark condition,  $t(27) = 0.28, p$   
 22  $= .78$ , Cohen's  $d = 0.07$ ,  $BF_{01} = 6.60$ . These results indicate no variance reduction. As described

1 in the Introduction (Equation 3), variance reduction is one of the two signatures of the Bayesian  
2 cue combination.

3 The mean SD in the Both condition was significantly larger than the mean optimal SD,  $t$   
4 (27) = 3.73,  $p < .01$ , Cohen's  $d = 1.00$ . The mean SD in the Conflict condition was significantly  
5 larger than the mean optimal SD,  $t$  (27) = 5.43,  $p < .001$ , Cohen's  $d = 1.45$ . The mean observed  
6 landmark weight (0.57) was not significantly different from the mean optimal landmark weight  
7 (0.37),  $t$  (27) = 2.05,  $p = .05$ , Cohen's  $d = 0.55$ ,  $BF_{01} = 1.03$ . These results indicate no minimum  
8 variance. As described in the Introduction (Equation 4), minimum variance is the other signature  
9 of the Bayesian cue combination.

10 **For the group of L2/L1=1**, the main effect of the cue condition was significant,  $F$  (3, 81)  
11 = 3.98,  $p < .05$ .  $MSE = 265.66$ ,  $\eta_p^2 = .13$ . Planned contrasts showed that the mean SD in the Both  
12 condition was not significantly different from that in the Path-Integration condition,  $t$  (27) =  
13 0.09,  $p = .93$ , Cohen's  $d = 0.02$ ,  $BF_{01} = 6.83$ . The mean SD in the Both condition was  
14 significantly smaller than that in the Landmark condition,  $t$  (27) = 2.68,  $p = .01$ , Cohen's  $d =$   
15 0.72. The mean SD in the Conflict condition was not significantly different from that in the Path-  
16 Integration condition,  $t$  (27) = 1.48,  $p = .15$ , Cohen's  $d = 0.40$ ,  $BF_{01} = 2.45$ . The mean SD in the  
17 Conflict condition was not significantly different from that in the Landmark condition,  $t$  (27) =  
18 1.17,  $p = .25$ , Cohen's  $d = 0.31$ ,  $BF_{01} = 3.59$ . These results indicate variance reduction for the  
19 Both condition but no reduction for the Conflict condition.

20 The mean SD in the Both condition was significantly larger than the mean optimal SD,  $t$   
21 (27) = 2.57,  $p = .02$ , Cohen's  $d = 0.69$ . The mean SD in the Conflict condition was significantly  
22 larger than the mean optimal SD,  $t$  (27) = 3.69,  $p < .01$ , Cohen's  $d = 0.99$ . The mean observed  
23 landmark weight (0.46) was not significantly different from the mean optimal landmark weight

1 (0.38),  $t(27) = 0.70$ ,  $p = .49$ , Cohen's  $d = 0.19$ ,  $BF_{01} = 5.43$ . These results indicate that no  
 2 minimum variance was produced.

3 **For the group of L2/L1=0.5**, the main effect of the cue condition was significant,  $F(3,$   
 4  $81) = 4.30$ ,  $p < .01$ .  $MSE = 340.39$ ,  $\eta_p^2 = .14$ . Planned contrasts showed that the mean SD in the  
 5 Both condition was significantly smaller than that in the Path-Integration condition,  $t(27) = 3.74$ ,  
 6  $p < .01$ , Cohen's  $d = 1.00$ . The mean SD in the Both condition was significantly smaller than  
 7 that in the Landmark condition,  $t(27) = 2.63$ ,  $p = .01$ , Cohen's  $d = 0.70$ . The mean SD in the  
 8 Conflict condition was significantly smaller than that in the Path-Integration condition,  $t(27) =$   
 9  $2.22$ ,  $p = .04$ , Cohen's  $d = 0.59$ . The mean SD in the Conflict condition was not significantly  
 10 different from that in the Landmark condition,  $t(27) = 1.42$ ,  $p = .17$ , Cohen's  $d = 0.38$ ,  $BF_{01} =$   
 11  $2.67$ . These results indicate variance reduction for the Both and Conflict conditions.

12 The mean SD in the Both condition was not significantly different from the mean optimal  
 13 SD,  $t(27) = 0.18$ ,  $p = .86$ , Cohen's  $d = 0.05$ ,  $BF_{01} = 6.75$ . The mean SD in the Conflict condition  
 14 was not significantly different from the mean optimal SD,  $t(27) = 0.66$ ,  $p = .52$ , Cohen's  $d =$   
 15  $0.18$ ,  $BF_{01} = 5.56$ . The mean observed landmark weight (0.65) was not significantly different  
 16 from the mean optimal landmark weight (0.56),  $t(27) = 0.63$ ,  $p = .54$ , Cohen's  $d = 0.17$ ,  $BF_{01} =$   
 17  $5.66$ . These results indicate that the minimum variance was produced.

### 18 **2.2.2 Heading errors**

19 The circular means of the heading errors (Table 1) showed clear biases for the Conflict  
 20 conditions in all of the leg ratio groups. According to the 95% confidence interval, the circular  
 21 means significantly differed from  $0^\circ$ .

1 SDs of heading errors were analyzed using mixed-model ANOVAs, with a within-  
 2 participant variable of the cue condition and a between-participant variable of the leg ratio.  
 3 Figure 7 plots the mean SDs of heading errors for the four cue conditions and the three different  
 4 leg ratios. Mean optimal SDs are also plotted.

5 The main effect of the cue condition was significant,  $F(3, 243) = 46.08, p < .001, MSE =$   
 6  $171.35, \eta_p^2 = .36$ . The main effect of the leg ratio was not significant,  $F(1, 81) = 2.14, p = .13,$   
 7  $MSE = 497.50, \eta_p^2 = .05$ . The interaction between the cue condition and leg ratio was not  
 8 significant,  $F(6, 243) = 1.83, p = .09, MSE = 171.35, \eta_p^2 = .04$ . Planned contrasts showed that  
 9 the mean SD in the Both condition was significantly smaller than that in the Path-Integration  
 10 condition,  $t(83) = 10.09, p < .001, Cohen's d = 1.56$ . The mean SD in the Both condition was  
 11 not significantly different from that in the Landmark condition,  $t(83) = 1.61, p = .11, Cohen's d$   
 12  $= 0.25, BF_{01} = 3.29$ . The mean SD in the Conflict condition was significantly smaller than that in  
 13 the Path-Integration condition,  $t(83) = 8.54, p < .001, Cohen's d = 1.32$ . The mean SD in the  
 14 Conflict condition was not significantly different from that in the Landmark condition,  $t(83) =$   
 15  $1.18, p = .24, Cohen's d = 0.18, BF_{01} = 5.87$ . These results indicate variance reduction for the  
 16 Both and Conflict conditions.

17 As there was no main effect of the leg ratio, mean SDs in the Both and Conflict  
 18 conditions across the leg ratio groups were compared with mean optimal SDs across the leg ratio  
 19 groups. The difference for the Both condition was not significant,  $t(83) = 1.05, p = .30, Cohen's$   
 20  $d = 0.16, BF_{01} = 6.74$ . The difference for the Conflict condition was not significant,  $t(83) = 1.78,$   
 21  $p = .08, Cohen's d = 0.27, BF_{01} = 2.51$ . The landmark weight was analyzed using mixed-model  
 22 ANOVAs, with a within-participant variable of the observed optimal difference (observed vs.  
 23 optimal) and a between-participant variable of the leg ratio. The main effect of the observed

1 optimal difference was not significant,  $F(1, 81) = 0.00, p = .99, MSE = 0.14, \eta_p^2 = .00$ . The main  
 2 effect of the leg ratio was not significant,  $F(1, 81) = 2.03, p = .14, MSE = 0.15, \eta_p^2 = .05$ . The  
 3 interaction between the observed optimal difference and leg ratio was not significant,  $F(1, 81) =$   
 4  $0.61, p = .54, MSE = 0.14, \eta_p^2 = .02$ . These results indicate that the minimum variance was  
 5 produced for the Both and Conflict conditions.

### 6 **2.2.3 Position angular errors**

7 SDs of position angular errors were analyzed using mixed-model ANOVAs, with a  
 8 within-participant variable of the cue condition and a between-participant variable of the leg  
 9 ratio. Figure 8 plots the mean SDs of homing errors for the four cue conditions and the three  
 10 different leg ratios.

11 The main effect of the cue condition was not significant,  $F(3, 243) = 1.91, p = .13, MSE$   
 12  $= 190.17, \eta_p^2 = .02$ . The main effect of the leg ratio was significant,  $F(1, 81) = 4.02, p = .02,$   
 13  $MSE = 701.22, \eta_p^2 = .09$ . The interaction between the cue condition and leg ratio was not  
 14 significant,  $F(6, 243) = 0.88, p = .51, MSE = 190.17, \eta_p^2 = .02$ . These results confirm that the  
 15 SDs of position estimates were the same across different cue conditions, consistent with our  
 16 conjecture that errors of position estimates in all of the cue conditions were attributed to errors  
 17 from path integration.

### 18 **2.2.4 Fit the model to observed homing angular variability**

19 We also tested whether the observed SDs of the homing angular errors ( $\theta$ ) could be  
 20 predicted by the mathematical model based on the self-localization hypothesis as listed in Table  
 21 A1 in Appendix 1.

1 For each participant, we conducted a linear regression between individual position  
 2 angular errors ( $\pi$ ) and heading errors ( $\eta$ ) across four paths in the Path-Integration condition.  
 3 Figure 9 plots the regression line for each participant and the mean regression line for each leg  
 4 ratio group. The mean coefficients (slope and intercept) and the squared mean Pearson  $r$  are also  
 5 presented in the figure. Mean slopes (0.79, 0.58, and 0.27 for L2/L1 = 2, 1, 0.5 respectively)  
 6 were significantly different across the three groups,  $F(2, 81) = 5.10, p < .01, MSE = 0.38, \eta_p^2$   
 7  $= .11$ . The mean Pearson  $r$ s (0.76, 0.57, and 0.49 for L2/L1 = 2, 1, 0.5 respectively) were  
 8 significantly different across the three groups,  $F(2, 81) = 3.30, p = .04, MSE = 0.16, \eta_p^2 = .08$ ,  
 9 and also different from 0 for all three groups,  $t_s(27) \geq 5.77, p_s < .001$ . These results support our  
 10 conjectures that the position error depends on the heading error ( $\pi_{PI} = a \times \eta_{PI}$ ) and the  
 11 dependency (slope  $a$  and  $r^2$ ) increases with the leg ratio.

12 For each leg ratio group, using the linear regression of heading error and position angular  
 13 error in the Path-Integration condition (Figure 9), we obtained the estimates of slope  $a$  and  $\sigma_{ue}^2$ ,  
 14 which is (mean observed SDs of position error) $^2 \times (1 - (\text{mean } r)^2)$ . Table 2 summarizes these  
 15 estimates.

16 Following the equations in Table A1B, we calculated the predicted homing SD in each  
 17 cue condition for each participant in each leg ratio group. Specifically, we used the observed  
 18 heading SD in the Path-Integration and Landmark conditions ( $\sigma_{\eta_{PI}}^2, \sigma_{\eta_{LM}}^2$ ) from each participant  
 19 and the group parameters including slope  $a$  and unexplained variability ( $\sigma_{ue}^2$ ) from the  
 20 corresponding group (Table 2). In addition, for the Both condition, we used the mean of the  
 21 optimal weight for heading estimations ( $W_{\eta_{PI}}, W_{\eta_{LM}}$ ) in each group, whereas for the Conflict  
 22 condition, we used the mean of the observed weight for heading estimations in the Conflict  
 23 condition in each group.

1           The mean observed and predicted SDs of homing angular errors for all cue conditions  
2 and all of the leg ratio groups are plotted in Figure 10. Mixed-model ANOVAs, with within-  
3 participant variables of the predicted observed difference (predicted vs. observed) and the cue  
4 condition, and a between-participant variable of the leg ratio, showed no main effect of the  
5 predicted observed difference,  $F(1, 81) = 0.16, p = .69, MSE = 486.00, \eta_p^2 < .01$ . There was no  
6 interaction between the predicted observed difference and any other variables. These results  
7 indicate that the model fit the data well.

8           We also contrasted the homing hypothesis with the self-localization hypothesis by  
9 examining their ability to explain the observed SDs of the homing angular error in the Both and  
10 Conflict conditions respectively. In particular, according to the homing hypothesis, the observed  
11 SDs of the homing angular errors in the two-cue conditions (Both and Conflict) should be the  
12 same as the optimal SDs of the homing angular errors. In contrast, according to the self-  
13 localization hypothesis, the observed SDs of the homing errors in the two-cue conditions should  
14 be the same as the predicted values using the mathematical model as described above. The  
15 models were fit by maximizing the likelihood of the data using the generalized linear mixed  
16 model in SPSS (IBM SPSS statistics, 2017). The fits were compared using the Bayesian  
17 Information Criterion (BIC), a common model comparison criterion. The BIC values for the  
18 homing hypothesis and the self-localization hypothesis are listed in Table 3. The difference in  
19 BIC values ( $\Delta BIC$ ) can be converted to an approximation of the BF,  $\ln(BF) = \Delta BIC/2$   
20 (Wagenmakers, 2007). As a result, BFs are also listed in Table 3.

21           The hypothesis with the smaller BIC is favored if the  $BF > 3$  (or  $BF < 1/3$ ) and strongly  
22 favored if the  $BF > 10$  (or  $BF < 1/10$ ) (Rouder et al., 2009). According to Table 3, the self-  
23 localization hypothesis is strongly favored by the data in the Both and Conflict conditions for the

1 group of  $L2/L1=2$ . The self-localization hypothesis is strongly favored by the data in the Conflict  
2 condition and is favored by the data in the Both condition for the group of  $L2/L1=1$ . There was  
3 no evidence to favor either hypothesis for the group of  $L2/L1=0.5$ .

4 Consistent with results of the comparisons that test variance reduction and minimum  
5 variance, the BFs also favor the mathematical model of the self-localization hypothesis over the  
6 homing hypothesis for the groups of  $L2/L1=2$  and  $L2/L1=1$ . The mathematical model predicts  
7 that the homing variability for the group of  $L2/L1=0.5$  appears to follow the Bayesian cue  
8 combination. Therefore, it is not surprising that the Bayes factors of the group of  $L2/L1=0.5$   
9 could not differentiate the mathematical model of the self-localization hypothesis from the  
10 homing hypothesis.

### 11 **2.3 Discussion**

12 In all of the leg ratio groups, the evidence of variance reduction and minimum variance  
13 was obtained for heading estimates, consistent with the Bayesian cue combination. The evidence  
14 consistent with the Bayesian cue combination for homing estimates was only clear in the group  
15 of  $L2/L1=0.5$  but not in the other two groups. These results favor the self-localization hypothesis  
16 over the homing hypothesis. Furthermore, it is difficult for the homing hypothesis to explain why  
17 the Bayesian model can explain the homing variability for the group of  $L2/L1=0.5$  but not for the  
18 other two groups. In contrast, the mathematical model based on the self-localization hypothesis  
19 can well explain all of these findings.

### 20 **3. Experiment 2**

21 The participants in Experiment 1 learned objects before walking a path and indicated the  
22 original locations of the objects after walking the path in order to calculate position errors and

1 heading errors. In contrast, a typical homing paradigm does not involve learning the locations of  
2 objects and replacing objects (Chen et al., 2017). Thus, the Experiment 1's conclusion may not  
3 be generalized to the typical homing paradigm. The purpose of Experiment 2 was to differentiate  
4 the self-localization hypothesis from the homing hypothesis in a typical homing paradigm. As the  
5 homing errors in the group of  $L2/L1=2$  clearly differentiate the self-localization hypothesis from  
6 the homing hypothesis, we only used  $L2/L1=2$  in this experiment. Without learning any of the  
7 objects' locations, the participants walked the paths with a leg ratio of 2 ( $L2/L1=2$ ) and then  
8 pointed to the origins of the paths in the four cue conditions. Note that, as in a typical homing  
9 paradigm, neither position nor heading estimates were derived or analyzed.

10         The participants did not learn any objects, which saved experimental time. Consequently,  
11 for each participant we doubled the number of paths (from four to eight) in each cue condition to  
12 reduce the variance in estimating circular means and SDs in all cue conditions.

### 13 **3.1 Methods**

#### 14 **3.1.1 Participants**

15         Twenty-eight university students (14 men and 14 women) participated in the experiment  
16 to fulfill a partial requirement for an introductory psychology course. Before the experiment, all  
17 participants signed the consent form approved by the University of Alberta Research Ethics  
18 Board.

#### 19 **3.1.2 Materials, Design, and Procedure**

20         Experiment 2 was similar to Experiment 1 except for the following changes. First, this  
21 experiment only included one leg ratio group ( $L2/L1 = 2$ ). Second, participants did not learn the  
22 locations of any objects or indicate the original locations of objects. After walking a path, they  
23 were asked to use the wand to point to the origin (O). Finally, there were eight, instead of four,

1 path configurations for each cue condition. While keeping the turning angles 50° and 130° in  
 2 Experiment 1, we added two more turning angles avoiding the right angle (90°). One is 30° larger  
 3 than 50° (i.e., 80°) and the other is 30° smaller than 130° (i.e., 100°).

### 4 **3.2 Results**

5 The circular mean of the homing angular errors (Table 1) showed a clear bias for the  
 6 Conflict condition. According to the 95% confidence interval, the circular mean significantly  
 7 differed from 0°.

8 A repeated measures ANOVA was used to analyze the cue effect on the homing angular  
 9 errors. Figure 11 plots the mean SDs for the four cue conditions and the mean optimal SD.

10 The main effect of the cue condition is significant,  $F(3, 81) = 12.23, p < .001$ .  $MSE =$   
 11  $198.40, \eta_p^2 = .31$ . Planned contrasts showed that the mean SD in the Both condition was  
 12 significantly larger than that in the Path-Integration condition,  $t(27) = 4.54, p < .01$ , Cohen's  $d =$   
 13  $1.21$ . The mean SD in the Both condition was not significantly different from that in the  
 14 Landmark condition,  $t(27) = 1.97, p = .06$ , Cohen's  $d = 0.53, BF_{01} = 1.18$ . The mean SD in the  
 15 Conflict condition was significantly larger than that in the Path-Integration condition,  $t(27) =$   
 16  $3.35, p < .01$ , Cohen's  $d = 0.89$ . The mean SD in the Conflict condition was significantly smaller  
 17 than that in the Landmark condition,  $t(27) = 3.44, p < 0.01$ , Cohen's  $d = 0.92$ . These results  
 18 indicate no variance reduction.

19 The mean SD in the Both condition was significantly larger than the mean optimal SD,  $t$   
 20  $(27) = 6.67, p < .001$ , Cohen's  $d = 1.78$ . The mean SD in the Conflict condition was significantly  
 21 larger than the mean optimal SD,  $t(27) = 5.90, p < .001$ , Cohen's  $d = 1.58$ . The mean observed  
 22 weight to assigned to the landmark cue (0.33) was not significantly different from the mean

1 optimal landmark weight (0.31),  $t(27) = 0.18$ ,  $p = .86$ , Cohen's  $d = 0.05$ ,  $BF_{01} = 6.75$ . These  
 2 results indicate that no minimum variance was produced.

### 3 **3.3 Discussion**

4 Experiment 2 replicated the result of no Bayesian combination in homing estimates for  
 5 the L2/L1=2 group in Experiment 1, indicating that this result is not specific to the paradigm of  
 6 learning the locations of objects.

7 It is important to note that Experiment 1 (and 2) provided a special situation to  
 8 distinguish between the homing hypothesis and the self-localization hypothesis. With the distal  
 9 landmarks, piloting cannot produce a positioning estimate, thus cannot produce a homing  
 10 estimate. Without two independent homing estimates to combine, is Experiment 1 still able to  
 11 test the homing hypothesis?<sup>9</sup>

12 We argue that Experiment 1 is still capable of testing the homing hypothesis by  
 13 examining the Bayesian cue combination in homing estimates. The homing hypothesis predicts  
 14 that piloting will not be functional to estimate the home in Experiment 1. Consequently, the  
 15 homing estimation for the Landmark condition will be random; homing estimations for the two-  
 16 cue conditions (Both and Conflict) will only rely on path integration (i.e. A weight of 1 is  
 17 assigned to home estimates from path integration). The relationships among homing variances  
 18 for all conditions can be written as  $\sigma_{\theta}^2_{\text{Both}} = \sigma_{\theta}^2_{\text{PI}}$ ,  $\sigma_{\theta}^2_{\text{Conflict}} = \sigma_{\theta}^2_{\text{PI}}$ ,  $\sigma_{\theta}^2_{\text{Landmark}} \gg \sigma_{\theta}^2_{\text{PI}}$ . From  
 19 these relationships, we still have  $\sigma_{\theta}^2_{\text{Both}} = \sigma_{\theta}^2_{\text{Conflict}} \leq \min(\sigma_{\theta}^2_{\text{PI}}, \sigma_{\theta}^2_{\text{Landmark}})$  (the variance  
 20 reduction criterion, see Equation 3). Because  $\sigma_{\theta}^2_{\text{Landmark}} \gg \sigma_{\theta}^2_{\text{PI}}$ , the optimal weight assigned to  
 21 path integration and variance for the two-cue conditions should be  $W_{PI} = 1$  and  $\sigma_{\theta}^2_{\text{Optimal}} = \sigma_{\theta}^2_{\text{PI}}$

---

<sup>9</sup> We are grateful to one anonymous reviewer for this suggestion.

1 (see Equation 4). Because  $\sigma_{\theta_{\text{Both}}}^2 = \sigma_{\theta_{\text{PI}}}^2, \sigma_{\theta_{\text{Conflict}}}^2 = \sigma_{\theta_{\text{PI}}}^2$ , and  $\sigma_{\theta_{\text{Optimal}}}^2 = \sigma_{\theta_{\text{PI}}}^2$ , we get  
 2  $\sigma_{\theta_{\text{Both}}}^2 = \sigma_{\theta_{\text{Conflict}}}^2 = \sigma_{\theta_{\text{Optimal}}}^2$  (the minimum variance criterion, see Equation 4). Thus, the  
 3 homing hypothesis can still be applied to Experiment 1 by incorporating the criteria of variance  
 4 reduction and minimum variance. Because the data in Experiment 1 did not fit these two criteria,  
 5 the homing hypothesis was disconfirmed in the situation when only path integration can indicate  
 6 the home.

7 We acknowledge that this conclusion may not necessarily be generalized to the situations  
 8 where both piloting and path integration can indicate the home. Experiments 3 and 4 addressed  
 9 this concern.

#### 10 **4. Experiment 3**

11 The purpose of Experiment 3 was to differentiate the self-localization hypothesis from  
 12 the homing hypothesis when the distal landmarks were replaced by proximal landmarks.  
 13 Although distal landmarks alone in the previous experiments are not able to indicate the home  
 14 locations, proximal landmarks alone could specify the home locations. As the estimated positions  
 15 were produced both from path integration and piloting, we also had opportunity to examine the  
 16 Bayesian combination for position estimates as well as for homing and heading estimates.

17 The mathematical model of the self-localization hypothesis assumes that distal landmarks  
 18 (indicating orientations but not positions) are used. However, conceptually, the model seems  
 19 applicable to situations when proximal landmarks are used. According to the model, when the leg  
 20 ratio is large (i.e.,  $L2/L1=2$ ), the position angular error ( $\pi_{PI}$ ) is strongly dependent on the  
 21 heading error ( $\eta_{PI}$ ) in path integration. These strongly dependent errors were cancelled out in  
 22 contributing to the homing angular error ( $\theta_{PI} = \pi_{PI} - \eta_{PI}$ ), yielding a very small homing

1 variability in the Path-Integration condition (See Figure A1A). It might be hard to observe an  
2 even smaller homing variability in the two-cue (Both/Conflict) conditions to produce evidence of  
3 variance reduction (one signature of the Bayesian combination) even when the proximal  
4 landmark is used.

## 5 **4.1 Method**

### 6 **4.1.1 Participants**

7 Twenty-eight university students (14 men and 14 women) participated in the experiment  
8 to fulfill a partial requirement for an introductory psychology course. Before the experiment, all  
9 participants signed the consent form approved by the University of Alberta Research Ethics  
10 Board.

### 11 **4.1.2 Materials, Design, and Procedure**

12 The materials, design, and procedure were the same as for those in the group of  $L2/L1=2$   
13 of Experiment 1 except for the following changes. The shapes (landmarks) were presented on a  
14 much smaller circular wall with a radius of 5m and a height of 1m instead of the 50m-radius  
15 circular wall in Experiment 1. Note that in Experiments 1 and 2, the distal landmarks alone only  
16 indicated participants' testing heading but not their testing positions. Thus, the rotation of the  
17 distal landmark, whether around the origin (i.e., O) or around the testing position (i.e., P), only  
18 affected estimates of headings but not positions. However, the proximal landmarks alone  
19 indicated the testing position. The rotation of the proximal landmarks around the origin (i.e., O)  
20 and around the testing position (i.e., P) would have different impacts on position estimates.  
21 Following the previous studies (e.g., Chen et al., 2017; Nardini et al., 2008), we varied the origin  
22 of the path (i.e., O), but kept the testing position (i.e., P) constant across paths (by switching O

1 and P in Figure 5F). The testing position was the same as the center of the wall so that the  
2 landmarks rotated around the testing position (P) in the Conflict condition.

## 3 **4.2 Results**

### 4 **4.2.1 Homing angular errors**

5 The circular mean of the homing angular errors (Table 1) showed a clear bias for the  
6 Conflict condition. According to the 95% confidence interval, the circular mean significantly  
7 differed from 0°.

8 A repeated measures ANOVA was used to analyze the cue effect on the homing angular  
9 errors. Figure 12 plots the mean SDs for the four cue conditions and the optimal SD. The main  
10 effect of the cue condition was not significant,  $F(3, 81) = 1.11, p = .35, MSE = 229.84, \eta_p^2 = .04$ .  
11 This indicates no variance reduction.

12 The mean SD in the Both condition was significantly larger than the mean optimal SD,  $t$   
13  $(27) = 2.52, p = .02$ , Cohen's  $d = 0.67$ . The mean SD in the Conflict condition was not  
14 significantly different from the mean optimal SD,  $t(27) = 1.96, p = .06$ , Cohen's  $d = 0.52$ ,  $BF_{01}$   
15  $= 1.19$ . The mean observed landmark weight (0.50) was not significantly different from the mean  
16 optimal landmark weight (0.54),  $t(27) = 0.22, p = .83$ , Cohen's  $d = 0.06$ ,  $BF_{01} = 6.69$ . These  
17 results indicate that no minimum variance was produced for the Both condition and there was no  
18 clear evidence for the Conflict condition.

### 19 **4.2.2 Heading errors**

20 The circular mean of the heading errors (Table 1) showed a clear bias for the Conflict  
21 condition. According to the 95% confidence interval, the circular mean significantly differed  
22 from 0°.

1 A repeated measures ANOVA analyzed the cue effect on the heading errors. Figure 13  
2 plots the mean SDs for the four cue conditions and the optimal SD.

3 The main effect of the cue condition was significant,  $F(3, 81) = 8.97, p < .001, MSE =$   
4  $309.14, \eta_p^2 = .25$ . Planned contrasts showed that the mean SD in the Both condition was  
5 significantly smaller than that in the Path-Integration condition,  $t(27) = 4.61, p < .001$ , Cohen's  
6  $d = 1.23$ . The mean SD in the Both condition was not significantly different from that in the  
7 Landmark condition,  $t(27) = 1.43, p = .16$ , Cohen's  $d = 0.38$ ,  $BF_{01} = 2.63$ . The mean SD in the  
8 Conflict condition was significantly smaller than that in the Path-Integration condition,  $t(27) =$   
9  $4.55, p < .001$ , Cohen's  $d = 1.22$ . The mean SD in the Conflict condition was not significantly  
10 different from that in the Landmark condition,  $t(27) = 1.21, p = .24$ , Cohen's  $d = 0.32$ ,  $BF_{01} =$   
11  $3.43$ . These results indicate a variance reduction for the Both and Conflict conditions.

12 The mean SD in the Both condition was not significantly different from the mean optimal  
13 SD,  $t(27) = 1.11, p = .28$ , Cohen's  $d = 0.30$ ,  $BF_{01} = 3.80$ . The mean SD in the Conflict condition  
14 was not significantly different from the mean optimal SD,  $t(27) = 1.31, p = .20$ , Cohen's  $d =$   
15  $0.35$ ,  $BF_{01} = 3.07$ . The mean observed landmark weight (0.72) was not significantly different  
16 from the mean optimal landmark weight (0.65),  $t(27) = 0.58, p = .57$ , Cohen's  $d = 0.16$ ,  $BF_{01} =$   
17  $5.82$ . These results indicate that the minimum variance was produced.

### 18 **4.2.3 Position angular errors**

19 A repeated measures ANOVA was used to analyze the cue effect on the position angular  
20 errors. Figure 14 plots the mean SDs of position angular errors for the four cue conditions. The  
21 main effect of the cue condition was not significant,  $F(3, 81) = 2.16, p = .10, MSE = 293.77, \eta_p^2$   
22  $= .07$ . These results indicate no variance reduction.

1           The mean SD in the Both condition was significantly larger than the mean optimal SD,  $t$   
2     (27) = 2.90,  $p = .007$ , Cohen's  $d = 0.78$ . The mean SD in the Conflict condition was significantly  
3     larger than the mean optimal SD,  $t$  (27) = 3.48,  $p = .002$ , Cohen's  $d = 0.93$ . These results indicate  
4     that no minimum variance was produced. Note that in the Conflict condition, the landmarks were  
5     rotated around the testing position (P), so there was no discrepancy between the testing positions  
6     predicted by path integration and piloting. Thus, we could not test whether participants used the  
7     optimal weight in position estimates.

### 8     **4.3 Discussion**

9           The evidence consistent with the Bayesian cue combination was obtained for heading  
10    estimates but not for homing estimates. These findings favor the self-localization hypothesis over  
11    the homing hypothesis even when the proximal landmarks replaced the distal landmarks in the  
12    previous experiments. These findings suggest that people combine self-localization estimates  
13    from piloting and from path integration but do not combine homing estimates even when both  
14    piloting and path integration can produce separate homing estimates.

15           Although the current study distinguishes between self-localization hypothesis and the  
16    homing hypothesis by primarily examining the Bayesian cue combination for heading and  
17    homing estimates to, it is worth noting that Experiment 3 did not provide evidence of the  
18    Bayesian cue combination for position estimates.

19           No Bayesian cue combination for position estimates might be due to the specific  
20    experiment design. In the Landmark condition, the participants were disoriented by spinning in  
21    place at the end of the path. As a result, disorientation could not disrupt the position estimate  
22    from path integration. As both path integration and piloting contributed to the position estimate

1 for the Landmark condition, this experiment may not be able to examine the cue combination for  
2 position estimations.

3 Experiment 4 addressed this issue. In addition, replicating findings for homing and  
4 heading estimates in Experiment 3 is important as Experiment 3 is the single experiment that  
5 showed **evidence consistent with the** Bayesian cue combination in heading estimates but not in  
6 homing estimates in situations when both piloting and path integration indicate the home.

## 7 **5. Experiment 4**

8 In Experiment 4, instead of disorienting the participants in the Landmark condition at the  
9 end of the path, we disoriented them at the turning position (T in Figure 5F, note that as in  
10 Experiment 3, O and P in Figure 5F were switched) of the two-leg path. As shown in past  
11 studies, path integration cannot produce accurate position estimates during any further walking  
12 after disorientation (Mou & Zhang, 2014). Therefore, participants only could use piloting in the  
13 Landmark condition. As the estimated positions were independent in the Path-Integration and  
14 Landmark conditions, this design could examine the Bayesian combination for position  
15 estimates.

### 16 **5.1 Method**

#### 17 **5.1.1 Participants**

18 Twenty-eight university students (14 men and 14 women) participated in the experiment  
19 to fulfill a partial requirement for an introductory psychology course. Before the experiment, all  
20 participants signed the consent form approved by the University of Alberta Research Ethics  
21 Board.

## 1 5.1.2 Materials, Design & Procedure

2 Experiment 4 was very similar to Experiment 3 except for the Landmark condition. The  
3 participants were disoriented at the turning position (T in Figure 5F). After disorientation they  
4 were asked to search for a green pole, which indicated the testing position (P), and walk towards  
5 it.

## 6 5.2 Results

### 7 5.2.1 Homing angular errors

8 The circular mean of the homing angular errors (Table 1) showed a clear bias for the  
9 Conflict condition. According to the 95% confidence interval, the circular mean significantly  
10 differed from 0°.

11 A repeated measures ANOVA was used to analyze the cue effect on the homing angular  
12 errors. Figure 12 plots the mean SDs for the four cue conditions and the optimal SD. The main  
13 effect of the cue condition was significant,  $F(3, 81) = 3.75, p < .05, MSE = 117.59, \eta_p^2 = .12$ .  
14 Planned contrasts showed that the mean SD in the Both condition was not significantly different  
15 from that in the Path-Integration condition,  $t(27) = 0.55, p = .59, \text{Cohen's } d = 0.15, BF_{01} = 5.93$ .  
16 The mean SD in the Both condition was not significantly different from that in the Landmark  
17 condition,  $t(27) = 0.56, p = .58, \text{Cohen's } d = 0.15, BF_{01} = 5.90$ . The mean SD in the Conflict  
18 condition was significantly larger than that in the Path-Integration condition,  $t(27) = 2.32, p$   
19  $< .05, \text{Cohen's } d = 0.62$ . The mean SD in the Conflict condition was significantly larger than that  
20 in the Landmark condition,  $t(27) = 2.72, p < .05, \text{Cohen's } d = 0.73$ . These results indicate no  
21 variance reduction.

22 The mean SD in the Both condition was significantly larger than the mean optimal SD,  $t$   
23  $(27) = 5.26, p < .001, \text{Cohen's } d = 1.41$ . The mean SD in the Conflict condition was significantly

1 larger than the mean optimal SD,  $t(27) = 5.55, p < .001$ , Cohen's  $d = 1.48$ . The mean observed  
 2 landmark weight (0.74) was significantly larger than the mean optimal landmark weight (0.49),  $t$   
 3  $(27) = 2.75, p < .05$ , Cohen's  $d = 0.73$ . These results indicate no minimum variance produced.

#### 4 **5.2.2 Heading errors**

5 The circular mean of the heading errors (Table 1) showed a clear bias for the Conflict  
 6 condition. According to the 95% confidence interval, the circular mean significantly differed  
 7 from  $0^\circ$ .

8 A repeated measures ANOVA analyzed the cue effect on the heading errors. Figure 13  
 9 plots the mean SDs for the four cue conditions and the optimal SD.

10 The main effect of the cue condition was significant,  $F(3, 81) = 4.78, p = .004$ .  $MSE =$   
 11  $328.01, \eta_p^2 = .15$ . Planned contrasts showed that the mean SD in the Both condition was  
 12 significantly smaller than that in the Path-Integration condition,  $t(27) = 3.44, p = .002$ , Cohen's  
 13  $d = 0.92$ . The mean SD in the Both condition was significantly smaller than that in the Landmark  
 14 condition,  $t(27) = 3.24, p = .003$ , Cohen's  $d = 0.87$ . The mean SD in the Conflict condition was  
 15 significantly smaller than that in the Path-Integration condition,  $t(27) = 2.12, p = .04$ , Cohen's  $d$   
 16  $= 0.57$ . The mean SD in the Conflict condition was not significantly different from that in the  
 17 Landmark condition,  $t(27) = 1.14, p = .26$ , Cohen's  $d = 0.31$ ,  $BF_{01} = 3.69$ . These results indicate  
 18 a variance reduction for the Both and Conflict conditions.

19 The mean SD in the Both condition was not significantly different from the mean optimal  
 20 SD,  $t(27) = 0.97, p = .34$ , Cohen's  $d = 0.26$ ,  $BF_{01} = 4.38$ . The mean SD in the Conflict condition  
 21 was not significantly different from the mean optimal SD,  $t(27) = 1.69, p = .10$ , Cohen's  $d =$   
 22  $0.45$ ,  $BF_{01} = 1.83$ . The mean observed landmark weight (0.70) was not significantly different

1 from the mean optimal landmark weight (0.56),  $t(27) = 1.16$ ,  $p = .26$ , Cohen's  $d = 0.31$ ,  $BF_{01} =$   
 2 3.62. These results indicate that the minimum variance was produced.

### 3 **5.2.3 Position angular errors**

4 A repeated measures ANOVA was used to analyze the cue effect on the position angular  
 5 errors. Figure 14 plots the mean SDs of position angular errors for the four cue conditions. The  
 6 main effect of the cue condition was significant,  $F(3, 81) = 2.65$ ,  $p = .05$ ,  $MSE = 339.61$ ,  $\eta_p^2$   
 7 = .09.

8 Planned contrasts showed that the mean SD in the Both condition was significantly  
 9 smaller than that in the Path-Integration condition,  $t(27) = 2.63$ ,  $p = .01$ , Cohen's  $d = 0.70$ . The  
 10 mean SD in the Both condition was not significantly different from that in the Landmark  
 11 condition,  $t(27) = 1.51$ ,  $p = .14$ , Cohen's  $d = 0.40$ ,  $BF_{01} = 2.38$ . The mean SD in the Conflict  
 12 condition was not significantly different from that in the Path-Integration condition,  $t(27) =$   
 13 1.39,  $p = .18$ , Cohen's  $d = 0.37$ ,  $BF_{01} = 2.75$ . The mean SD in the Conflict condition was not  
 14 significantly different from that in the Landmark condition,  $t(27) = 0.11$ ,  $p = .91$ , Cohen's  $d =$   
 15 0.03,  $BF_{01} = 6.81$ . These results indicate a variance reduction for the Both but not for Conflict  
 16 conditions.

17 The mean SD in the Both condition was not significantly different from the mean optimal  
 18 SD,  $t(27) = 1.61$ ,  $p = .12$ , Cohen's  $d = 0.43$ ,  $BF_{01} = 2.07$ . The mean SD in the Conflict condition  
 19 was significantly larger than the mean optimal SD,  $t(27) = 2.60$ ,  $p = .02$ , Cohen's  $d = 0.69$ .  
 20 These results indicate that minimum variance was produced for the Both but not for the Conflict  
 21 conditions.

### 1 **5.3 Discussion**

2           The findings of this experiment replicated **evidence consistent with** the Bayesian cue  
3 combination for heading estimates but not for homing estimates in Experiment 3, further  
4 favoring the self-localization hypothesis over the homing hypothesis in the situation when  
5 proximal landmarks indicate the home.

6           For the position estimations, we also find **evidence consistent with** the Bayesian  
7 combination for the Both condition. Note that the landmarks rotated with respect to the testing  
8 position (P) in the Conflict condition. As a result, there were no conflicting predictions for the  
9 position estimates. Hence, analyzing the Bayesian combination for the Conflict condition is not  
10 conclusive.

## 11 **6. General Discussion**

12           The purpose of the current study was to investigate when the Bayesian cue combination  
13 of piloting and path integration occurs in human homing behaviors. The self-localization  
14 hypothesis stipulated that the Bayesian cue combination would occur when the participants were  
15 estimating their self-localization. The homing hypothesis stipulated that the Bayesian cue  
16 combination would occur when the participants were estimating their home location. The  
17 findings of all four experiments showed **evidence consistent with the Bayesian cue combination**  
18 for heading estimates for all leg ratios and both landmark types (distal or proximal), but **no**  
19 **evidence consistent with the** Bayesian cue combination for homing estimates in the leg-ratio-of-2  
20 group regardless of the landmark type. Thus, these findings favor the self-localization hypothesis  
21 over the homing hypothesis.

1           Although there was evidence consistent with the Bayesian cue combination in the homing  
2 estimations for the leg-ratio-of-0.5 group in Experiment 1, it is very hard for the homing  
3 hypothesis to explain why people combine homing estimates for a small leg ratio ( $L2/L1=0.5$ )  
4 but not for a large leg ratio ( $L2/L1=1$  and  $2$ ). By contrast, the mathematical model of the self-  
5 localization hypothesis clearly predicted that the Bayesian cue combination for heading estimates  
6 could lead to the variance reduction for homing estimates when the leg ratio was small but would  
7 lead to no reduction (even increase) for homing estimates when the leg ratio was large. Indeed,  
8 as illustrated by Figure 10, the mathematical model of the self-localization hypothesis clearly  
9 explained the observed homing variability in the group with the leg ratio of 0.5 as well as other  
10 leg ratio groups ( $L2/L1=1$  and  $L2/L1=2$ ). Therefore, the overall findings of the current study  
11 favor the self-localization hypothesis over the homing hypothesis.

12           One may be concerned that evidence favoring the self-localization hypothesis over the  
13 homing hypothesis in Experiments 1, 3, and 4 was specific to the experiment paradigm used. The  
14 participants learned objects at the origin of the path and indicated the locations of the objects at  
15 the end of the path. This experimental paradigm was very different from the typical homing  
16 paradigm used in previous studies (Chen et al., 2017; Nardini et al., 2008). This concern was  
17 partially addressed by the finding in Experiment 2. Similar to the typical homing paradigm, the  
18 participants walked the path with a leg ratio of 2 ( $L2/L1=2$ ) and pointed to the origin without  
19 learning any object array in Experiment 2. The results still showed the absence of the Bayesian  
20 cue combination for the homing estimations. Therefore, evidence favoring the self-localization  
21 hypothesis over the homing hypothesis in Experiments 1, 3, and 4 is not specific to the paradigm  
22 of learning locations of objects.

1           The self-localization hypothesis was consistent with findings in non-human studies. For  
2 example, head direction cells and place cells can be activated by both landmarks and inertial cues  
3 (Taube, 2007). The self-localization hypothesis was also consistent with previous human studies  
4 showing that visual landmarks reset heading or position estimates from path integration (Mou &  
5 Zhang, 2014; Zhang & Mou, 2017). However, no prior study has examined the Bayesian cue  
6 combination in both self-localization estimations (i.e., heading/position estimations) and homing  
7 estimations. For the first time, the current study demonstrates that for human adults, the Bayesian  
8 cue combination occurs in self-localization estimations rather than in homing estimations.

9           Previous studies showed that homing estimations of human adults could be explained by  
10 the Bayesian cue combination model (e.g., Chen et al., 2017; Nardini et al., 2008; Sjolund et al.,  
11 2018; but see Zhao & Warren, 2015). We speculate that these findings might have occurred  
12 because these studies used various leg ratios and analyzed the data by collapsing all leg ratios. In  
13 the current study, evidence for the Bayesian cue combination for homing estimates existed when  
14 the leg ratio was 0.5 but not when the leg ratio was 2. Evidence in the group with the leg ratio of  
15 1 was in between (e.g. variance reduction but no minimum variance for the Both condition).  
16 Thus, it would be possible to obtain the evidence of the Bayesian cue combination if collapsed  
17 data across all leg ratios had been analyzed in the previous studies. We acknowledge our  
18 paradigm of Experiment 2 was similar but not identical to the paradigm used in the past studies  
19 (Nardini et al., 2008). Hence, it is plausible that the Bayesian cue combination model may work  
20 in the exact paradigm of the past work. Future studies should examine this possibility.  
21 Nevertheless, the findings of the current study at least suggest that we should examine  
22 heading/position estimations in addition to homing estimations when we study cue interaction in  
23 human navigation.

1           We note that in the current study, variance reduction for the heading estimates in the  
2 both-cue conditions occurred relative to the Path-Integration condition in Experiments 1 and 3  
3 (variance reduction relative to the Landmark condition was also observed in Experiment 4). We  
4 speculate that when the heading estimation variability from landmarks is much smaller than that  
5 from path integration, the estimation variability in the two-cue conditions may not be  
6 significantly smaller than that in the Landmark condition. The other explanation is that in the  
7 two-cue conditions, participants might have only used the heading estimates from piloting and  
8 ignored the estimates from path integration in the manner of the landmark dominance cue  
9 combination reported by Zhao & Warren (2015). The landmark dominance cue combination  
10 specifies that the landmark weight is the value of one whereas the path integration weight is the  
11 value of zero (Zhao & Warren, 2015). We compared the mean of the observed landmark weight  
12 for heading estimates in the Conflict conditions to 1 for all experiments. As illustrated in Table 4,  
13 all comparisons but one ( $L2/L1 = 0.5$  in Experiment 1) indicated that the mean of the observed  
14 landmark weights was significantly smaller than 1. These findings suggest that the participants  
15 might have weighed cues in the Bayesian manner rather than a landmark dominance cue  
16 combination.

17           Similarly, it is interesting to test whether a landmark dominance cue combination can  
18 explain the observed homing variability as suggested by by Zhao and Warren (2015). We  
19 compared the mean of the observed landmark weight for homing estimations (homing angular  
20 errors) in the Conflict conditions to 1 for all experiments. As illustrated in Table 4, all  
21 comparisons indicated that the mean of the observed landmark weights was significantly smaller  
22 than 1. Consequently, these findings do not agree with the landmark dominance cue combination  
23 for homing estimations, which was possible as reported by Zhao and Warren (2015).

1           It is important to note that although the primary purpose of the current study was to  
2 examine the stage in which the Bayesian cue combination between path integration and piloting  
3 occurs, the more general question is when *cue interaction*, including cue combination and cue  
4 competition (i.e., landmark dominance, Zhao & Warren, 2015), occurs. To dissociate the self-  
5 localization hypothesis from the homing hypothesis, we used a rather small angular distance in  
6 the Conflict condition (45°) so that the Bayesian cue combination could occur either for heading  
7 estimations or homing estimations. The findings suggest that the Bayesian cue combination  
8 occurs in self-localization estimations prior to homing estimations. However, we never exclude  
9 the possibility of cue competition in self-localization estimations. As we discussed in the  
10 Introduction, cue competitions (i.e., landmark dominance) in heading/position estimations were  
11 reported in our previous studies (Mou & Zhang, 2014; Zhang & Mou, 2017; see also Zhao &  
12 Warren, 2015). In addition, we note that the 2D shapes (i.e., a circle, rectangle, and polygon)  
13 used as landmarks in the current study are relatively weak orientation cues. They might have  
14 encouraged participants to also use cues from path integration rather than only use landmark cues  
15 as reported by Zhang and Warren (2015). Indeed, any evidence of cue competition, just like the  
16 Bayesian cue combination, in heading estimations but not in homing estimations, supports rather  
17 than undermines the self-localization hypothesis.

18           Some findings in previous studies have already challenged the possibility that a *real* cue  
19 competition occurs at homing estimations. For example, Zhao and Warren (2015) reported that  
20 the mean of the homing estimates in the Conflict condition was determined by landmark only,  
21 whereas variances of the homing estimates in the Both and Conflict conditions were smaller than  
22 those in the single-cue conditions. A *real* cue competition model specifying landmark dominance  
23 would predict not only that the mean of the observed homing errors in the Conflict condition was

1 determined by landmark only (i.e., landmark weight = 1) but also that the observed homing  
2 variability in the Conflict condition should be the same as that in the Landmark condition.  
3 Hence, the reduced (smaller) variability in the Conflict condition relative to single-cue  
4 conditions in Zhao and Warren's study was at odds with a *real* cue combination model for  
5 homing estimates.

6         Elaborating on the self-localization hypothesis, we developed a mathematical model that  
7 quantitatively describes how people use path integration and piloting to guide homing behavior  
8 when distal landmarks are used (see Table A1). As far as we know, for the first time, a  
9 mathematical model quantitatively describing the relations between position, heading, and  
10 homing errors in terms of variability has been proposed and empirically confirmed. This model  
11 accurately predicted homing angular variability in Experiment 1 (Figure 10). The regression  
12 analyses shown in Figure 9 clearly support the assumption that the position error linearly  
13 depends on the heading error in path integration and that the dependency increases with the leg  
14 ratio. Furthermore, the simulation based on this model in Figure A1 predicts that when L2/L1  
15 increases, the homing variability in the Both condition more likely departs from the prediction  
16 based on the Bayesian cue combination and may be even larger than the homing variability in the  
17 Path-Integration condition. This prediction was confirmed by the finding in Experiment 1  
18 (Figure 6, L2/L1=2).

19         In the current study, to easily contrast the homing and the self-localization hypotheses,  
20 we only systematically examined the Bayesian cue combination for the heading error and the  
21 homing error but not the position error. We deliberately made the position errors in all cue  
22 conditions were the same in Experiments 1 and 2. We also disoriented participants in the  
23 Landmark condition in Experiment 3, so did not remove the position representation from path

1 integration in the Landmark condition. In addition, we rotated landmarks with respect to the  
2 participants' testing position in the Conflict condition (Chen et al., 2017; Nardini et al., 2008;  
3 Zhao & Warren, 2015). This manipulation objectively made the heading and homing estimates  
4 from piloting and path integration in the Conflict condition discrepant in a predicted degree (i.e.,  
5 45°). However, it did not create discrepant estimates for the position estimates. Therefore, we  
6 could not systematically test the cue combination model in position estimations. Although  
7 Experiment 4 showed the preliminary evidence of the Bayesian cue combination for position  
8 estimates, future studies should systematically test the Bayesian cue combinations for position  
9 estimations as well as for heading and homing estimations.

10         Following the previous studies, which investigated cue combinations in human  
11 navigation (e.g., Nardini et al., 2008), the current study only used two-leg outbound paths before  
12 participants made responses. It also used a relatively simple environment. In real-life navigation,  
13 individuals often navigate by walking much more complicated paths (e.g., Baronchelli &  
14 Radicchi, 2013) in much more complex environments. We speculate that people still combine  
15 estimates produced by path integration and piloting in self-localization prior to homing (and  
16 localizing other invisible goals). However, the cue weights in combination might vary according  
17 to the reliability and stability of cues that people perceive in each specific navigation situation  
18 (Chen et al., 2017; Wang, Mou, & Dixon, 2018). Future studies should test the generalizability of  
19 the self-localization hypothesis.

20         Last but not least, although more evidence favoring the self-localization hypothesis over  
21 the homing hypothesis, we should be cautious to decisively conclude that heading estimates  
22 exactly follow the Bayesian cue combination. The strongest evidence of the Bayesian cue  
23 combination should show variance reduction relative to both single cue conditions. However, in

1 the current study, only Experiment 4 showed this evidence. Experiments 1 and 3 showed  
2 variance reduction relative to the Path-Integration condition but not the Landmark condition, the  
3 ambiguous category according to Rohde et al. (2016). This ambiguous situation is attributed to  
4 the fact of a much more precise heading estimate based on the landmarks than based on the path  
5 integration in the current study. Indeed, this fact might have provided the best opportunity  
6 differentiating the self-localization hypothesis from the homing hypothesis with a large distance  
7 between the weights producing the largest variance reduction for heading and homing estimates  
8 (see Figure A1 and Equation A5). Future studies should use more similar variance of heading  
9 estimates based on single cues to conclusively test the Bayesian cue combination for heading  
10 estimates.

11 In conclusion, the current findings support the self-localization hypothesis in human  
12 homing behaviors. People combine self-localization estimates (positions/headings estimates)  
13 from piloting and path integration and then use the combined self-localization estimates to  
14 determine the home location.

15

## References

- 1  
2 Baronchelli, A., & Radicchi, F. (2013). Lévy flights in human behavior and cognition. *Chaos,*  
3 *Solitons & Fractals, 56*, 101-105.
- 4 Benhamou, S., Sauv e, J. P., & Bovet, P. (1990). Spatial memory in large scale movements:  
5 efficiency and limitation of the egocentric coding process. *Journal of Theoretical*  
6 *Biology, 145*(9), 1-12.
- 7 Butler, J. S., Smith, S. T., Campos, J. L., & B ulhoff, H. H. (2010). Bayesian integration of visual  
8 and vestibular signals for heading. *Journal of vision, 10*(11), 23-23.
- 9 Chen, X., McNamara, T. P., Kelly, J.W., & Wolbers, T. (2017). Cue combination in human spatial  
10 navigation. *Cognitive Psychology, 95*, 105-144.
- 11 Cheng, K., Shettleworth, S. J., Huttenlocher, J., & Rieser, J. J. (2007). Bayesian integration of  
12 spatial information. *Psychological Bulletin, 133*, 625–637.
- 13 Chrastil, E.R., & Warren, W.H. (2014). From cognitive maps to cognitive graphs. *PLoS ONE*  
14 *9*(11): e112544. doi:10.1371/journal.pone.0112544
- 15 Ernst, M. O., & Banks, M. S. (2002). Humans integrate visual and haptic information in a  
16 statistically optimal fashion. *Nature, 415*, 429–433.
- 17 Etienne, A. S., & Jeffery, K. J. (2004). Path integration in mammals. *Hippocampus, 14*(2), 180-  
18 192.
- 19 Etienne, A. S., Maurer, R., Berlie, J., Reverdin, B., Rowe, T., Georgakopoulos, J., & S equinot, V.  
20 (1998). Navigation through vector addition. *Nature, 396*(6707), 161-164.

- 1 Etienne, A. S., Maurer, R., Boulens, V., Levy, A., & Rowe, T. (2004). Resetting the path  
2 integrator: A basic condition for route-based navigation. *The Journal of Experimental*  
3 *Biology*, 207, 1491–1508.
- 4 Foo, P., Warren, W. H., Duchon, A., & Tarr, M. J. (2005). Do humans integrate routes into a  
5 cognitive map? Map-versus landmark-based navigation of novel shortcuts. *Journal of*  
6 *Experimental Psychology: Learning, Memory, and Cognition*, 31(2), 195-215.
- 7 Freas, C. A. Narendra, A., & Cheng K. (2017). Compass cues used by a nocturnal bull ant,  
8 *Myrmecia midas*. *Journal of Experimental Biology*, 220, 1578-1585.
- 9 Friedman, A., & Kohler, B. (2003). Bidimensional regression: assessing the configural similarity  
10 and accuracy of cognitive maps and other two-dimensional data sets. *Psychological*  
11 *methods*, 8(4), 468.
- 12 Fujita, N., Klatzky, R. L., Loomis, J. M., & Golledge, R. G. (1993). The encoding-error model of  
13 pathway completion without vision. *Geographical Analysis*, 25, 295-314.
- 14 Fujita, N., Loomis, J. M., Klatzky, R. L., & Golledge, R. G. (1990). A minimal representation for  
15 dead-reckoning navigation: Updating the homing vector. *Geographical Analysis*, 22(4),  
16 324-335.
- 17 Gallistel, C. R. (1990). *The organization of learning*. Cambridge, MA: MIT Press
- 18 Gallistel, C. R., & Matzel, L. D. (2013). The neuroscience of learning: beyond the Hebbian  
19 synapse. *Annual Review of Psychology*, 64, 169-200.
- 20 Geva-Sagiv, M., Las, L., Yovel, Y., & Ulanovsky, N. (2015). Spatial cognition in bats and rats:  
21 from sensory acquisition to multiscale maps and navigation. *Nature Reviews*  
22 *Neuroscience*, 16(2), 94.

- 1 Klatzky, R. L. (1998). Allocentric and egocentric spatial representations: Definitions,  
2 distinctions, and interconnections. In *Spatial cognition* (pp. 1-17). Springer, Berlin,  
3 Heidelberg.
- 4 Körding, K.P., Beierholm, U., Ma, W.J., Quartz, S., Tenenbaum, J.B., & Shams, L. (2007).  
5 Causal inference in multisensory perception. *PLoS ONE* 2(9): e943.
- 6 Loomis, J. M., Klatzky, R. L., Golledge, R. G., Cicinelli, J. G., Pellegrino, J. W., & Fry, P. A.  
7 (1993). Nonvisual navigation by blind and sighted: Assessment of path integration ability.  
8 *Journal of Experimental Psychology: General*, 122(1), 73-91.
- 9 Loomis, J. M., Klatzky, R. L., Golledge, R. G., & Philbeck, J. W. (1999). Human navigation by  
10 path integration. In R. G. Golledge (Ed.), *Wayfinding: Cognitive mapping and other*  
11 *spatial processes* (pp. 125-151). Baltimore: Johns Hopkins.
- 12 Mittelstaedt, M. L., & Mittelstaedt, H. (1980). Homing by path integration in a  
13 mammal. *Naturwissenschaften*, 67(11), 566-567.
- 14 Maurer, R., & Séguinot, V. (1995). What is modelling for? a critical review of the models of  
15 path integration. *Journal of Theoretical Biology*, 175(4), 457-475.
- 16 Mou, W., & Wang, L. (2015). Piloting and path integration within and across boundaries. *Journal*  
17 *of Experimental Psychology: Learning, Memory, and Cognition*, 41(1), 220-234.
- 18 Mou, W., & Zhang, L. (2014). Dissociating position and heading estimation: rotated visual  
19 orientation cues perceived after walking reset headings but not positions. *Cognition*, 133,  
20 553-571.
- 21 Muller, R. (1996). A quarter of a century of place cells. *Neuron*, 17(5), 813-822.
- 22 Nardini, M., Jones, P., Bedford, R., & Braddick, O. (2008). Development of cue integration in  
23 human navigation. *Current Biology*, 18(9), 689-693.

- 1 Petrini, K., Caradonna, A., Foster, C., Burgess, N., & Nardini, M. (2016). How vision and self-  
2 motion combine or compete during path reproduction changes with age. *Scientific*  
3 *reports*, 6, 29163.
- 4 Rohde, M., van Dam, L. C. J., & Ernst, M. O. (2016). Statistically optimal multisensory cue  
5 integration: A practical tutorial. *Multisensory Research*, 29(4-5), 279-492.
- 6 Rouder, J. N., Speckman, P. L., Sun, D., Morey, R. D., & Iverson, G. (2009). Bayesian t tests for  
7 accepting and rejecting the null hypothesis. *Psychonomic bulletin & review*, 16(2), 225-  
8 237.
- 9 Sjolund, L. A., Kelly, J. W., & McNamara, T. P. (2018). Optimal combination of environmental  
10 cues and path integration during navigation. *Memory & Cognition*, 46, 89-99.
- 11 Taube, J. S. (2007). The head direction signal: origins and sensory-motor integration. *Annual*  
12 *Review of Neuroscience*, 30, 181-207.
- 13 Tcheang, L., Bühlhoff, H. H., & Burgess, N. (2011). Visual influence on path integration in  
14 darkness indicates a multimodal representation of large-scale space. *Proceedings of the*  
15 *National Academy of Sciences*, 108(3), 1152-1157.
- 16 Tolman, E. C. (1948). Cognitive maps in rats and men. *Psychological review*, 55(4), 189-208.
- 17 Tversky, B. (1993). Cognitive maps, cognitive collages, and spatial mental models. In A.U.  
18 Frank & I. Campari (Eds.), *Spatial information theory a theoretical basis for GIS* (pp. 14-  
19 24). Berlin: Springer.
- 20 Vickerstaff, R. J., & Cheung, A. (2010). Which coordinate system for modelling path  
21 integration? *Journal of Theoretical Biology*, 263(2), 242-261.
- 22 Wagenmakers, E. J. (2007). A practical solution to the pervasive problems of p  
23 values. *Psychonomic Bulletin & Review*, 14(5), 779-804.

- 1 Wang, L., Mou, W., & Dixon, P. (2018). Cue interaction between buildings and street  
2 configurations during reorientation in familiar and unfamiliar outdoor  
3 environments. *Journal of Experimental Psychology: Learning, Memory, and*  
4 *Cognition, 44(4)*, 631.
- 5 Wang, R. F., & Spelke, E. S. (2002). Human spatial representation: Insights from animals. *Trends*  
6 *in Cognitive Sciences, 6(9)*, 376-382.
- 7 Wehner, R., Michel, B., & Antonsen, P. (1996). Visual navigation in insects: coupling of  
8 egocentric and geocentric information. *Journal of Experimental Biology, 199(1)*, 129-  
9 140.
- 10 Zhang, H., Mou, W., & McNamara, T. P. (2011). Spatial updating according to a fixed reference  
11 direction of a briefly viewed layout. *Cognition, 119(3)*, 419-429.
- 12 Zhang, L., & Mou, W. (2017). Piloting systems reset path integration systems during position  
13 estimation. *Journal of Experimental Psychology: Learning, Memory and Cognition,*  
14 *43(3)*, 472-491.
- 15 Zhang, L., & Mou, W. (2019). Selective resetting position and heading estimations while driving  
16 in a large-scale immersive virtual environment. *Experimental brain research, 237(2)*,  
17 335-350.
- 18 Zhao, M., & Warren, W. H. (2015). How you get there from here: Interaction of visual landmarks  
19 and path integration in human navigation. *Psychological Science, 26(6)*, 915-924.

## 1 **Appendix 1: Mathematical model of the self-localization hypothesis**

2 According to the self-localization hypothesis, a cue combination occurs when the  
3 navigator estimates his/her position and heading. The combined position errors and combined  
4 heading errors then affect homing errors according to  $\theta = \pi - \eta$  (See Equation 5). As a result,  
5 the following equation describes the general format of the self-localization hypothesis;

$$6 \quad \theta = (W_{\pi_{PI}} \times \pi_{PI} + W_{\pi_{LM}} \times \pi_{LM}) - (W_{\eta_{PI}} \times \eta_{PI} + W_{\eta_{LM}} \times \eta_{LM}) \quad (A1)$$

7 To simplify the model, we designed experiments so that in all cue conditions, the position  
8 error was only from path integration (i.e.,  $W_{\pi_{PI}} = 1, W_{\pi_{LM}} = 0$ ). Therefore, Equation A1 can be  
9 simplified to the following equation.

$$10 \quad \theta = \pi_{PI} - (W_{\eta_{PI}} \times \eta_{PI} + W_{\eta_{LM}} \times \eta_{LM}) \quad (A2)$$

11 Equation A2 can be used for each cue condition with specific weights in heading  
12 combinations (i.e.,  $W_{\eta_{LM}}$ ). We list the specific format of Equation A2 for each cue condition in  
13 Table A1A.

14 We assume that the position error ( $\pi_{PI}$ ) and the heading error ( $\eta_{PI}$ ) from path integration  
15 follow a linear relationship:

$$16 \quad \pi_{PI} = a \times \eta_{PI} + ue \quad (A3)$$

17  $ue$  is the unexplained error, which is the portion of the position error that cannot be  
18 explained by the heading error from path integration. There are several possible reasons for the  
19 unexplained error: it could be due to a distance estimation error while walking the legs; or it  
20 could be due to other random errors in calculating position estimates from the lengths of the two  
21 legs and the turning angle (i.e., the heading).

1  $a$  is the slope of the linear relationship. Slope  $a$  is assumed to increase with the leg ratio  
 2 (e.g.,  $a$  is 0, 0.5, and 1 for a leg ratio of 0, 1, and  $\infty$ , respectively, see Figure 4).

3 Replacing  $\pi_{PI}$  in Equation A2 with  $a \times \eta_{PI} + ue$  according to Equation A3, we obtain  
 4 the last equation of the mathematical model.

$$5 \quad \theta = (a \times \eta_{PI} + ue) - (W_{\eta_{PI}} \times \eta_{PI} + W_{\eta_{LM}} \times \eta_{LM}) \quad (A4)$$

6 Using the specific weights for each cue condition, we list the specific format of Equation  
 7 A4 for each cue condition in Table A1A. Note that when  $W_{\eta_{PI}}$  is not 0, both  $\pi$  (i.e.,  $a \times \eta_{PI} +$   
 8  $ue$ ) and  $\eta$  (i.e.,  $W_{\eta_{PI}} \times \eta_{PI} + W_{\eta_{LM}} \times \eta_{LM}$ ) have  $\eta_{PI}$ . This shared portion of  $\eta_{PI}$  of  $\pi$  and  $\eta$  is  
 9 cancelled out in calculating  $\theta$  and  $\sigma_{\theta}^2$ .

10 We then calculate the variance of the predicted  $\theta$  ( $\sigma_{\theta}^2$ ) based on Equation A4 for each cue  
 11 condition.  $a$  is the slope of the linear regression between the observed heading error and position  
 12 error in the Path-Integration condition.  $ue \sim N(0, \sigma_{ue}^2)$ .  $\sigma_{ue}^2$  is the unexplained portion of the  
 13 variance of the observed position error in the linear regression ( $\sigma_{ue}^2 = \sigma_{\pi_{PI}}^2 \times (1 - r^2)$ ).  $\eta_{PI}$   
 14  $\sim N(0, \sigma_{\eta_{PI}}^2)$ ,  $\eta_{LM} \sim N(0, \sigma_{\eta_{LM}}^2)$ .  $\sigma_{\eta_{PI}}^2$  and  $\sigma_{\eta_{LM}}^2$  are the observed variance of heading errors in  
 15 the conditions of Path-Integration and Landmark respectively. Furthermore,  $ue$ ,  $\eta_{PI}$ , and  $\eta_{LM}$  are  
 16 independent of each other. In Table A1B, we specify all individual errors and their variances for  
 17 all cue conditions.

18 Consequently, we have all specifications of the mathematical model of the self-  
 19 localization hypothesis.

## 1 **Appendix 2: Manipulation of the ratio of the lengths of two legs (L2/L1)**

2 To dissociate the self-localization hypothesis from the homing hypothesis, we are seeking  
 3 evidence of a reduction in the variability of the heading error ( $\sigma_{\eta_{\text{Both}}}^2 \leq \min(\sigma_{\eta_{\text{PI}}}^2, \sigma_{\eta_{\text{LM}}}^2)$ ) but not  
 4 in the variability of the homing error ( $\sigma_{\theta_{\text{Both}}}^2 > \min(\sigma_{\theta_{\text{PI}}}^2, \sigma_{\theta_{\text{LM}}}^2)$ ) as a result of the cue  
 5 combination for heading estimates. As shown in Table A1B, both these variabilities  
 6 ( $\sigma_{\eta_{\text{Both}}}^2, \sigma_{\theta_{\text{Both}}}^2$ ) are a function of landmark weight used in the heading combination ( $W_{\eta_{\text{LM}}}$ ).  
 7 Therefore, we are seeking a situation in which  $W_{\eta_{\text{LM}}}$  could lead to a reduction in  $\sigma_{\eta_{\text{Both}}}^2$  but no  
 8 reduction in  $\sigma_{\theta_{\text{Both}}}^2$ . In short, we are seeking a situation in which the  $W_{\eta_{\text{LM}}}$  for  
 9 the minimum  $\sigma_{\eta_{\text{Both}}}^2$  is far from the  $W_{\eta_{\text{LM}}}$  for the minimum  $\sigma_{\theta_{\text{Both}}}^2$ . When these two landmark  
 10 weights are far from each other, the landmark weight in the heading estimation that reduces the  
 11 heading variability is less likely to simultaneously reduce the homing variability.

12 To implement this insight, we calculate the  $W_{\eta_{\text{LM}}}$  that leads to the minimum heading  
 13 variability in the two-cue condition (Both or Conflict). What we do is to find the minimum of  
 14  $\sigma_{\eta}^2 = W_{\eta_{\text{PI}}}^2 \times \sigma_{\eta_{\text{PI}}}^2 + W_{\eta_{\text{LM}}}^2 \times \sigma_{\eta_{\text{LM}}}^2$ . It turns out to be  $W_{\eta_{\text{LM}}} = \frac{\sigma_{\eta_{\text{PI}}}^2}{\sigma_{\eta_{\text{LM}}}^2 + \sigma_{\eta_{\text{PI}}}^2}$ . We refer to this weight  
 15 as the optimal landmark weight in the heading estimation (optimal  $W_{\eta_{\text{LM}}}$ ). We also calculate the  
 16  $W_{\eta_{\text{LM}}}$  that leads to the minimum homing variability in the Both or Conflict condition. What we  
 17 do is to find the minimum of  $\sigma_{\theta}^2 = (a - W_{\eta_{\text{PI}}})^2 \times \sigma_{\eta_{\text{PI}}}^2 + W_{\eta_{\text{LM}}}^2 \times \sigma_{\eta_{\text{LM}}}^2 + \sigma_{ue}^2$ . It turns out to be  
 18  $W_{\eta_{\text{LM}}} = \frac{\sigma_{\eta_{\text{PI}}}^2 \times (1-a)}{\sigma_{\eta_{\text{LM}}}^2 + \sigma_{\eta_{\text{PI}}}^2}$ , or  $(1 - a) \times \text{optimal } W_{\eta_{\text{LM}}}$ . Therefore, the distance between these two  
 19 landmark weights (referred to as Distance-of-Weight) can be calculated according to the  
 20 following equation:

$$21 \quad \text{Distance-of-Weight} = a \times \text{optimal } W_{\eta_{\text{LM}}} \quad (\text{A5})$$

1 As shown in the equation, Distance-of-Weight increases with slope  $a$ . A larger Distance-  
 2 of-Weight means a lower likelihood of simultaneously obtaining the reduction of homing  
 3 variability and heading variability. Thus using a larger slope, while we observe the Bayesian cue  
 4 combination in heading variability, we are less likely to observe the Bayesian combination in  
 5 homing variability, dissociating the self-localization hypothesis from the homing hypothesis.

6 To further illustrate these insights, we conduct a simulation based on the equations of  
 7  $\sigma_{\eta}^2$ ,  $\sigma_{\pi}^2$ , and  $\sigma_{\theta}^2$  in Table A1B (see the Matlab codes of this simulation at  
 8 <https://doi.org/10.7939/R3QB9VM6J>). This simulation assumes that the variability of the  
 9 heading error is much smaller from piloting than from path integration (i.e.,  $\sigma_{\eta_{LM}}^2/\sigma_{\eta_{PI}}^2 = 0.25$ ), as  
 10 distal landmarks may produce a much more precise heading estimate than path integration  
 11 (Taube, 2007; Zhao & Warren, 2015). This simulation also assumes that the variance of  $ue$  is  
 12 minimum (i.e.,  $\sigma_{ue}^2 = 0$ )<sup>10</sup>. Three different assumed values of  $a$  (i.e., 0.66, 0.5, and 0.33) are  
 13 used. As a result of the simulation, Figure A1 plots the predicted standard deviation (SD) for  
 14 each error in the two-cue condition (Both or Conflict) as a function of the landmark weight that  
 15 is used in combining heading estimates (i.e.,  $W_{\eta_{LM}}$ ).

16 In general, the findings of this simulation indicate that for the heading variability, the  
 17 largest reduction (i.e., the minimum SD) occurs when the landmark weight is 0.8 (the optimal  
 18 landmark weight for heading estimation, which is the red dot on the x axis in Figure A1)  
 19 regardless of slope  $a$ . Importantly, the landmark weight in heading estimations that produces the  
 20 minimum SD of homing errors (see the green dot on the x axis in Figure A1; values are 0.27, 0.4,  
 21 and 0.54 for Figures A1A, A1B, and A1C respectively) depends on slope  $a$ . Note that with an

---

<sup>10</sup> The conclusion from the simulation does not depend on the assumption that  $\sigma_{ue}^2 = 0$ , because  $\sigma_{ue}^2$  is constant and independent of the landmark weight in the heading estimation.

1 increase of slope  $a$ , the distance between the landmark weights for the minimum SD of homing  
2 errors (green dots) and for the minimum SD of heading errors (red dots) increases (0.53, 0.4,  
3 0.26 for Figures A1A, A1B, and A1C respectively), consistent with Equation A5 (i.e., slope  $a \times$   
4 0.8). Therefore, with a larger  $a$ , we are less likely to obtain the reduction of the homing  
5 variability while the heading variability is reduced by the cue combination in heading estimates.

6         Indeed, with a larger  $a$ , the homing variability due to the Bayesian combination for  
7 heading estimates (indicated by the red square in Figure A1A), could even be larger than the  
8 homing variability only from path integration (i.e., the SD of the homing error when the  
9 landmark weight is 0). Consequently, combining heading estimates from path integration and  
10 piloting to reduce the heading variability could increase (rather than reduce) the homing  
11 variability compared to the path integration condition. This is inconsistent with the Bayesian cue  
12 combination for homing estimations.

13         As discussed above (see Figure 4), slope  $a$ , the slope of the linear relationship between  
14 the position error and heading error from path integration, increases with the leg ratio ( $L2/L1$ ).  
15 Therefore, we could dissociate the self-localization hypothesis from the homing hypothesis by  
16 manipulating the leg ratio. These two hypotheses are more likely to be distinguished with a  
17 larger leg ratio.

*Table 1.* The circular mean of participants' observed circular means of homing angular errors ( $\theta$ ) and heading errors ( $\eta$ ) across paths in the Conflict condition and its 95% confidence interval (CI) in all experiments. The circular mean of homing angular errors predicted by the landmark is  $-45^\circ$  (i.e.,  $315^\circ$ ). The circular mean of heading angular errors predicted by the landmark is  $45^\circ$ .

	Experiment	Circular mean	95% CI
Homing angular errors	Exp 1: L2/L1 = 2	$334.62^\circ$	$[328.09^\circ, 341.14^\circ]$
	Exp 1: L2/L1 = 1	$339.42^\circ$	$[329.29^\circ, 349.55^\circ]$
	Exp 1: L2/L1 = 0.5	$331.75^\circ$	$[322.09^\circ, 341.40^\circ]$
	Exp 2 (L2/L1 = 2)	$345.17^\circ$	$[338.92^\circ, 351.42^\circ]$
	Exp 3 (L2/L1 = 2)	$334.94^\circ$	$[323.14^\circ, 346.74^\circ]$
	Exp 4 (L2/L1 = 2)	$326.75^\circ$	$[319.42^\circ, 334.07^\circ]$
Heading errors	Exp 1: L2/L1 = 2	$29.85^\circ$	$[23.54^\circ, 36.16^\circ]$
	Exp 1: L2/L1 = 1	$31.09^\circ$	$[22.22^\circ, 39.97^\circ]$
	Exp 1: L2/L1 = 0.5	$38.18^\circ$	$[29.55^\circ, 46.80^\circ]$
	Exp 3 (L2/L1 = 2)	$35.42^\circ$	$[24.79^\circ, 46.05^\circ]$
	Exp 4 (L2/L1 = 2)	$32.29^\circ$	$[21.48^\circ, 43.10^\circ]$

*Table 2.* Values of the squared mean observed SD of position angular errors ( $\pi$ ) in the Path-Integration condition ((mean observed SD of  $\pi_{PI}$ )<sup>2</sup>), the slope of the regression line between the position angular error and heading error ( $\eta$ ) in the Path-Integration condition ( $a$ ), the explained portion of the regression model (mean  $r$ )<sup>2</sup>, and variance of the unexplained error ( $\sigma_{ue}^2$ ) for the three leg ratio groups in Experiment 1.  $\sigma_{ue}^2 = (\text{mean observed SD of } \pi_{PI})^2 \times (1 - (\text{mean } r)^2)$ .

Leg ratio	$a$	(mean observed SD of $\pi_{PI}$ ) <sup>2</sup>	(mean $r$ ) <sup>2</sup>	$\sigma_{ue}^2$
L2/L1 = 2	0.79	1095.24	0.57	470.32
L2/L1 = 1	0.58	1290.55	0.33	869.16
L2/L1 = 0.5	0.27	606.32	0.23	469.31

*Table 3.* BIC values in explaining the observed SDs of homing angular errors ( $\theta$ ) for the conditions of Both and Conflict with the predicted SDs based on different hypotheses and the Bayes Factors (self-localization hypothesis over homing hypothesis) for all leg ratio groups in Experiment 1.

Leg ratio	Cue condition	BIC		Bayes Factor (likelihood ratio)
		Self-localization hypothesis	Homing hypothesis	
L2/L1 = 2	Both	702.63	718.95	3498.19
	Conflict	658.6	688.84	3685806.80
L2/L1 = 1	Both	699.31	702.48	4.88
	Conflict	714.78	726.43	338.66
L2/L1 = 0.5	Both	649.13	648.98	0.93
	Conflict	704.44	705.03	1.34

Table 4. Comparisons between the observed landmark weights and the value of one assuming landmark dominance in the heading estimations and the homing estimations.

	Experiment	Observed weight	<i>t</i>	<i>p</i>	Cohen's <i>d</i>
Heading estimations	Exp 1: L2/L1 = 2	0.66	4.70	< .001	1.26
	Exp 1: L2/L1 = 1	0.69	2.97	< .01	0.79
	Exp 1: L2/L1 = 0.5	0.86	1.41	0.17	0.38
	Exp 3 (L2/L1 = 2)	0.72	2.11	0.04	0.57
	Exp 4 (L2/L1 = 2)	0.70	2.40	0.02	0.64
Homing estimations	Exp 1: L2/L1 = 2	0.57	5.76	< .001	1.54
	Exp 1: L2/L1 = 1	0.46	4.64	< .001	1.24
	Exp 1: L2/L1 = 0.5	0.65	3.16	0.004	0.85
	Exp 2 (L2/L1 = 2)	0.33	9.33	< .001	2.49
	Exp 3 (L2/L1 = 2)	0.50	3.55	0.001	0.95
	Exp 4 (L2/L1 = 2)	0.74	3.06	0.005	0.82

*Table A1A.* The specific formats of Equations A2 and A4 for different cue conditions in Experiment 1 by assigning  $W_{\eta_{LM}} = 0$  to the Path-Integration condition and  $W_{\eta_{LM}} = 1$  to the Landmark condition.  $\theta$ ,  $\pi$ , and  $\eta$  are the homing angular error, position angular error, and heading error respectively.  $W_{\eta_{LM}}$  is the landmark weight and  $W_{\eta_{PI}}$  is the weight assigned to path integration in combining heading estimates ( $W_{\eta_{LM}} + W_{\eta_{PI}} = 1$ ).  $ue$  is the unexplained error and  $a$  is the slope of the linear relationship between the heading error and position angular error from path integration. 45 in the Conflict condition is the systematic error for heading estimates because the landmarks were rotated  $-45^\circ$ .

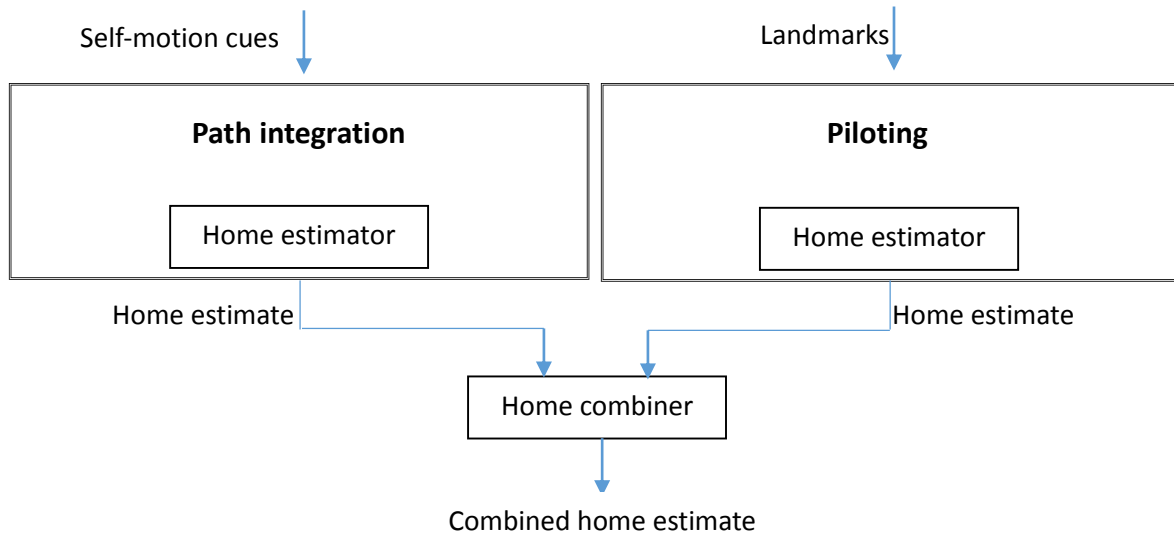
	Path-Integration (PI)	Landmark (LM)	Both	Conflict
Equation A2	$\theta = \pi_{PI} - \eta_{PI}$	$\theta = \pi_{PI} - \eta_{LM}$	$\theta = \pi_{PI} - (W_{\eta_{PI}} \times \eta_{PI} + W_{\eta_{LM}} \times \eta_{LM})$	$\theta = \pi_{PI} - (W_{\eta_{PI}} \times \eta_{PI} + W_{\eta_{LM}} \times (\eta_{LM} + 45))$
Equation A4	$\theta = a \times \eta_{PI} + ue - \eta_{PI}$	$\theta = a \times \eta_{PI} + ue - \eta_{LM}$	$\theta = a \times \eta_{PI} + ue - (W_{\eta_{PI}} \times \eta_{PI} + W_{\eta_{LM}} \times \eta_{LM})$	$\theta = a \times \eta_{PI} + ue - (W_{\eta_{PI}} \times \eta_{PI} + W_{\eta_{LM}} \times (\eta_{LM} + 45))$

*Table A1B.* Heading error, position angular error, homing angular error, and their variances in different cue conditions predicted by the mathematical model elaborating on the self-localization hypothesis.

	Path-Integration (PI)	Landmark (LM)	Both	Conflict
Heading error ( $\eta$ )	$\eta_{PI}$	$\eta_{LM}$	$W_{\eta_{PI}} \times \eta_{PI} + W_{\eta_{LM}} \times \eta_{LM}$	$W_{\eta_{PI}} \times \eta_{PI} + W_{\eta_{LM}} \times (\eta_{LM} + 45)$
Position error ( $\pi$ )	$a \times \eta_{PI} + ue$	$a \times \eta_{PI} + ue$	$a \times \eta_{PI} + ue$	$a \times \eta_{PI} + ue$
Homing error ( $\theta$ )	$(a - 1) \times \eta_{PI} + ue$	$a \times \eta_{PI} + ue - \eta_{LM}$	$(a - W_{\eta_{PI}}) \times \eta_{PI} + ue - W_{\eta_{LM}} \times \eta_{LM}$	$(a - W_{\eta_{PI}}) \times \eta_{PI} + ue - W_{\eta_{LM}} \times (\eta_{LM} + 45)$
$\sigma_\eta^2$	$\sigma_{\eta_{PI}}^2$	$\sigma_{\eta_{LM}}^2$	$W_{\eta_{PI}}^2 \times \sigma_{\eta_{PI}}^2 + W_{\eta_{LM}}^2 \times \sigma_{\eta_{LM}}^2$	$W_{\eta_{PI}}^2 \times \sigma_{\eta_{PI}}^2 + W_{\eta_{LM}}^2 \times \sigma_{\eta_{LM}}^2$
$\sigma_\pi^2$	$a^2 \times \sigma_{\eta_{PI}}^2 + \sigma_{ue}^2$	$a^2 \times \sigma_{\eta_{PI}}^2 + \sigma_{ue}^2$	$a^2 \times \sigma_{\eta_{PI}}^2 + \sigma_{ue}^2$	$a^2 \times \sigma_{\eta_{PI}}^2 + \sigma_{ue}^2$
$\sigma_\theta^2$	$(a - 1)^2 \times \sigma_{\eta_{PI}}^2 + \sigma_{ue}^2$	$a^2 \times \sigma_{\eta_{PI}}^2 + \sigma_{\eta_{LM}}^2 + \sigma_{ue}^2$	$(a - W_{\eta_{PI}})^2 \times \sigma_{\eta_{PI}}^2 + W_{\eta_{LM}}^2 \times \sigma_{\eta_{LM}}^2 + \sigma_{ue}^2$	$(a - W_{\eta_{PI}})^2 \times \sigma_{\eta_{PI}}^2 + W_{\eta_{LM}}^2 \times \sigma_{\eta_{LM}}^2 + \sigma_{ue}^2$

*Figure 1.* Schematic diagrams of the two hypotheses. **(A)** Homing hypothesis. **(B)** Self-localization hypothesis. The boxes of path integration and piloting indicate the two navigation processes. Each process receives the input of self-motion cues or landmarks and produces estimates. According to the homing hypothesis, each process produces an independent home estimate. According to the self-localization hypothesis, each process produces independent estimates of positions and headings. The boxes of estimators produce estimates. The boxes of combiners combine individual estimates.

### A. Homing hypothesis



### B. Self-localization hypothesis

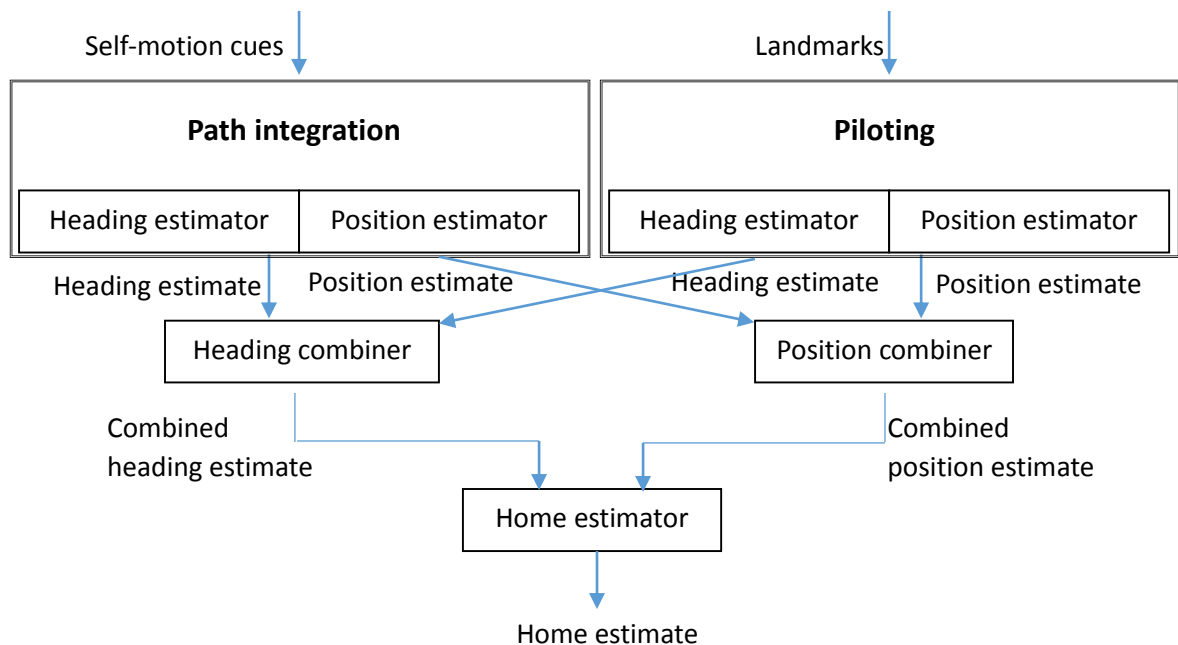
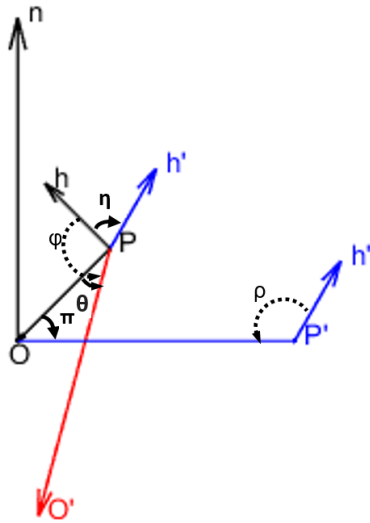
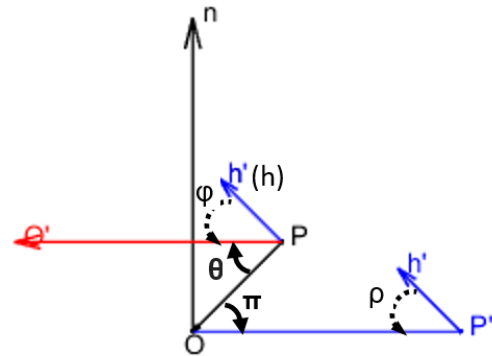


**Figure 2. (A)** A hypothetical participant represents his or her original position  $O$  (home) and heading  $n$ . After navigation, this participant ends at the position  $P$  and with the heading  $h$ . His or her estimates of  $P$  and  $h$  are  $P'$  and  $h'$ . He or she points to  $O'$  as the estimate of  $O$ . The angle  $\varphi$  from  $h$  to  $\overrightarrow{PO'}$  is the pointing direction. The angle  $\rho$  from  $h'$  to  $\overrightarrow{P'O'}$  is the remembered direction. These two directions are equal ( $\varphi = \rho$ ) assuming that the pointing direction follows the remembered direction. All angular errors for homing, position, and heading estimates are specified by the angular differences between the estimated and correct vectors or headings. Homing angular error ( $\theta$ ) is the angle from  $\overrightarrow{PO}$  to  $\overrightarrow{PO'}$ . Position angular error ( $\pi$ ) is the angle from  $\overrightarrow{OP}$  to  $\overrightarrow{OP'}$ . Heading error ( $\eta$ ) is the angle from the direction  $h$  to the direction  $h'$ . **(B)** Suppose there is only position error  $\pi$ .  $h = h'$  (i.e.  $\eta = 0$ ). As  $\varphi = \rho$  and  $h = h'$ , lines  $PO'$  and  $P'O'$  are parallel. Thus,  $\theta = \pi$ . **(C)** Suppose there is only heading error  $\eta$ .  $P' = P$  (i.e.,  $\pi = 0$ ). As  $\varphi - \theta = \rho + \eta$  and  $\varphi = \rho$ ,  $\theta = -\eta$ . **(D)** Suppose there are both errors  $\pi$  and  $\eta$ . Let  $\overrightarrow{PL} = \overrightarrow{P'O'}$ . Thus,  $\angle OPL = \pi$  (see panel B). The angle  $\rho$  equals the angle from  $h'$  to  $\overrightarrow{PL}$ . As  $\varphi - \angle LPO' = \rho + \eta$  and  $\varphi = \rho$ ,  $\angle LPO' = -\eta$  (see panel C).  $\theta = \angle OPL + \angle LPO' = \pi - \eta$ . We get equation 5. Conceptually, if we were to consider only the contribution of  $\pi$ , participants would point to  $L$  instead of  $O'$  ( $\theta_1 = \pi$ ). With the additional  $\eta$ , participants point to  $O'$  instead of  $L$  ( $\theta_2 = -\eta$ ).  $\theta = \theta_1 + \theta_2$ .

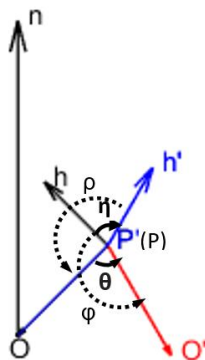
A.



B.



C.



D.

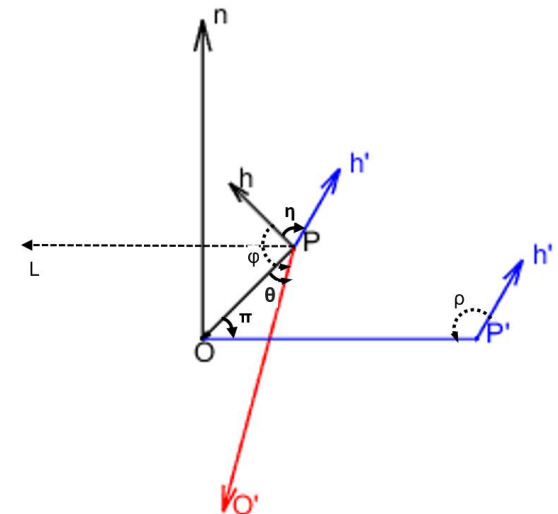


*Figure 3.* Illustrations of using the bidimensional regression to calculate estimated positions and headings. A participant learns five objects in the original locations (e.g., O). After navigation, the participant replaces objects from the testing position P and heading  $h$ . Conceptually, the bidimensional regression produces a prediction function (a transformation matrix including uniform scale, rotation, and translation). The prediction function converts the replaced locations (e.g., O') to the predicted locations so that the predicted locations overall have the shortest distance to the original locations (e.g., O) (Friedman & Kohler, 2003). The prediction function then calculates  $h'$  and P' using  $h$  and P as the values of the predictor respectively. The locations are connected by lines only to highlight the configuration of them so that the correspondences among the three configurations are clear to readers.

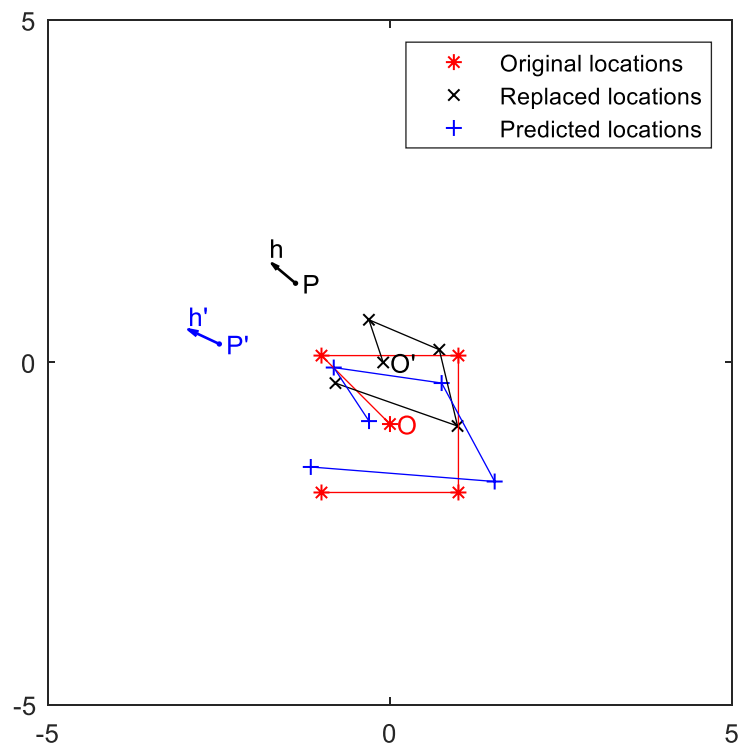


Figure 4. Illustrations of the relationship between the position angular error ( $\pi$ ) and the heading angular error ( $\eta$ ) from path integration. A participant walks from O to T (the first leg, L1) and turns at T, and walks from T to P (the second leg, L2), facing  $h$ . P' and  $h'$  are the estimates of the testing position (P) and heading ( $h$ ). This individual estimates the turning angle at T with an error, which is equal to the heading error ( $\eta$ ). (A) Participants do not walk Leg 2 (i.e., L2 is 0).  $L2/L1 = 0$ ,  $\pi = 0 \times \eta$ . (B) Participants walk the same distance for Legs 1 and 2.  $L2/L1 = 1$ ,  $\pi = 0.5 \times \eta$ . Because  $2 \times \angle TOP' + \angle P'TO = 180$  and  $2 \times \angle TOP + \angle PTO = 180^\circ$ , we get  $2 \times (\angle TOP' - \angle TOP) = \angle PTO - \angle P'TO$ .  $2 \times \pi = \eta$ . (C) Leg 2 is much longer than Leg 1 (similar to L1 is 0).  $L2/L1 = \infty$ ,  $\pi = 1 \times \eta$ .

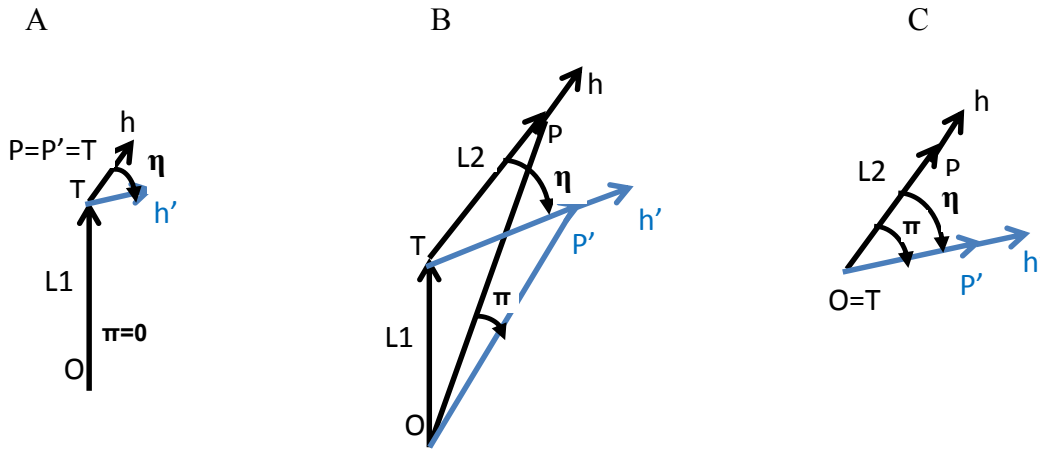


Figure 5. Virtual environment and path configurations in Experiment 1. (A) Learning position O (also the home), and the distal landmarks (a circle, polygon, and rectangle attached to the wall with a radius of 50m). (B) Testing position P, and testing heading  $h$ , in the Conflict condition with counter-clockwise rotated landmarks. (C) The array of the five objects learned at O. (D, E, & F) The four paths (O-T-P) were respectively used in three different leg ratio groups. (D:  $L2/L1=2$ ; E:  $L2/L1=1$ ; F:  $L2/L1=0.5$ ). Each P indicates one possible testing position at end of the second leg. Grid squares represent  $1m^2$ .

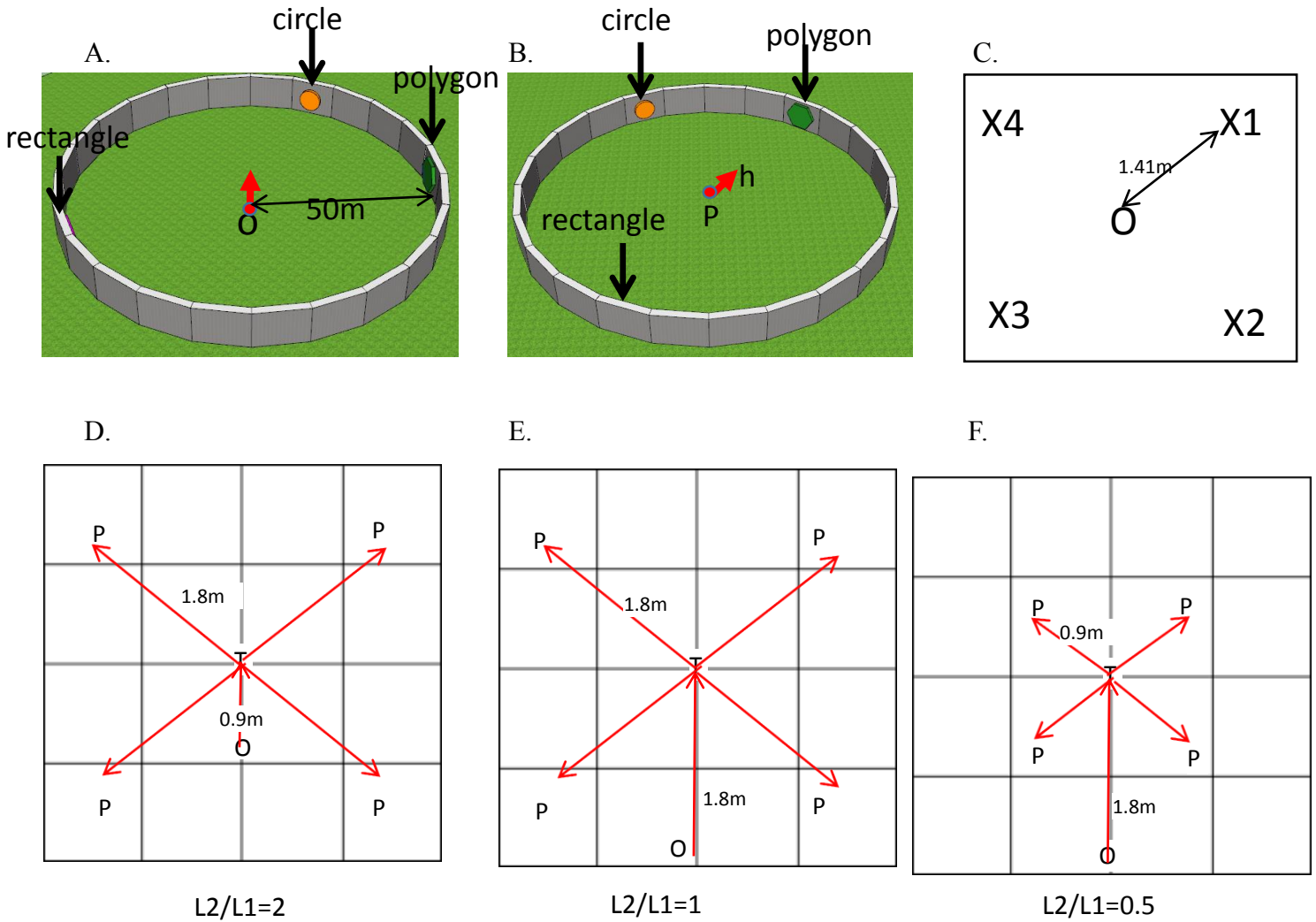


Figure 6. Mean observed SDs of the homing angular errors ( $\theta$ ) in the Path-Integration (PI), Landmark (LM), Both, and Conflict conditions, the optimal prediction by the Bayesian combination model (Optimal) when  $L2/L1 = 2, 1,$  and  $0.5$  in Experiment 1. Error bars represent  $\pm 1$  SE.

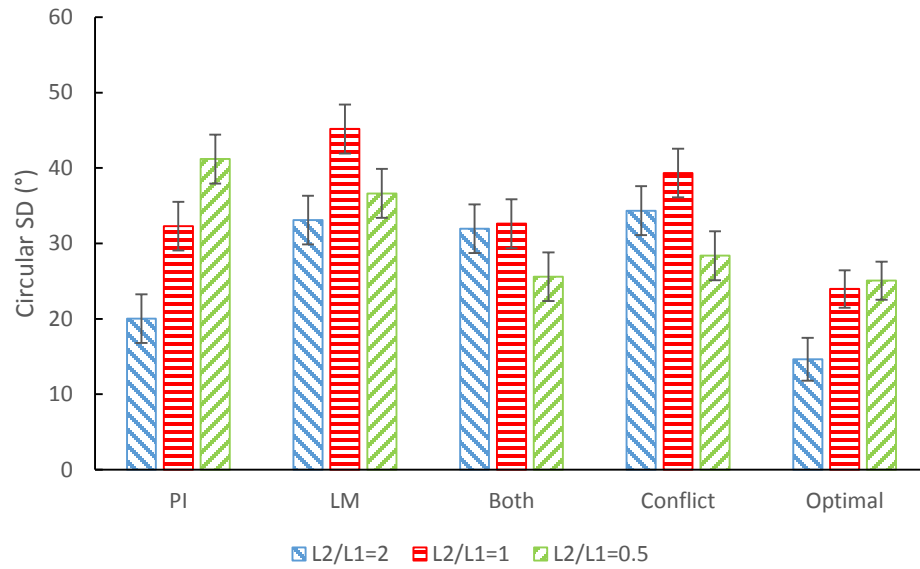


Figure 7. Mean observed SDs of the heading errors ( $\eta$ ) in the Path-Integration (PI), Landmark (LM), Both, and Conflict conditions, the optimal prediction by the Bayesian combination model (Optimal) when  $L2/L1 = 2, 1,$  and  $0.5$  in Experiment 1. Error bars represent  $\pm 1$  SE.

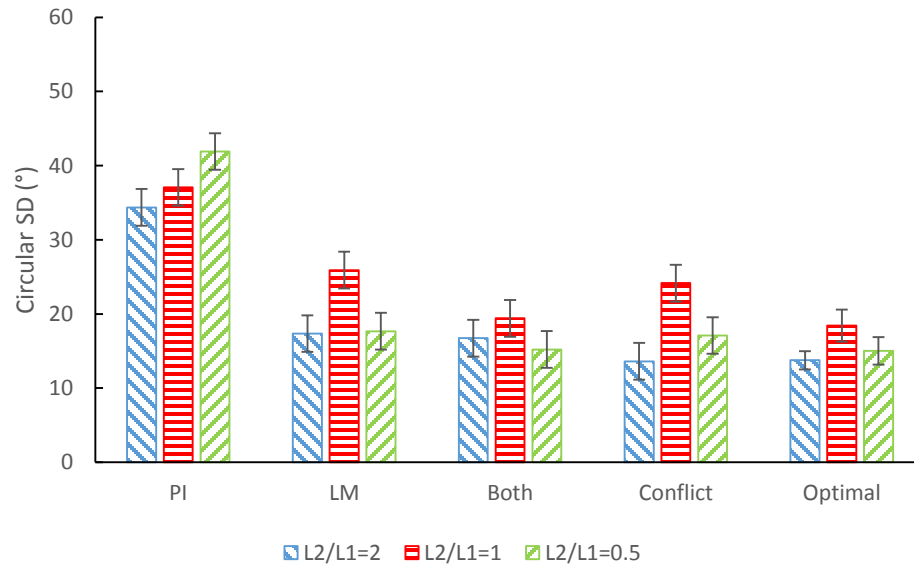


Figure 8. Mean observed SDs of the position angular errors ( $\pi$ ) in the Path-Integration (PI), Landmark (LM), Both, and Conflict conditions when L2/L1 = 2, 1, and 0.5 in Experiment 1. Error bars represent  $\pm 1$  SE.

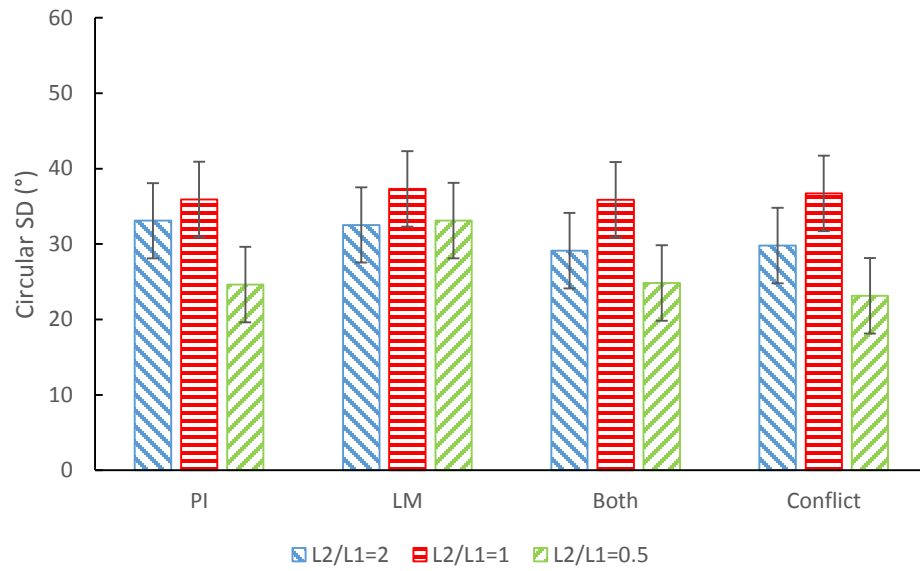
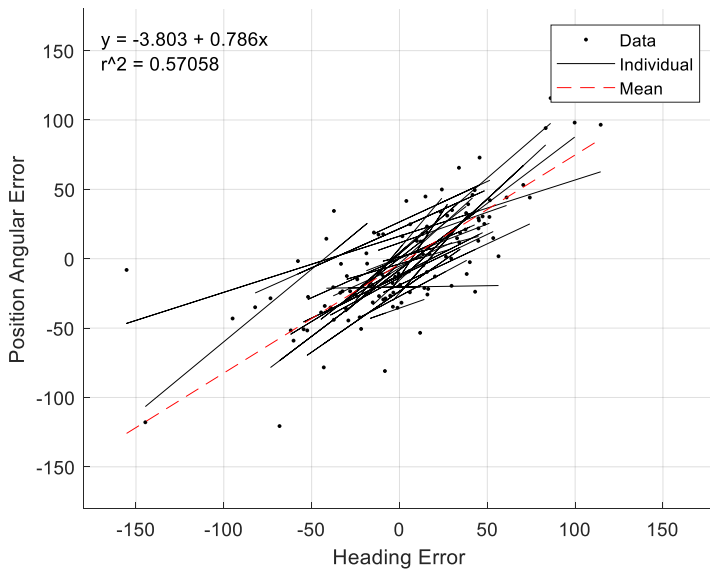
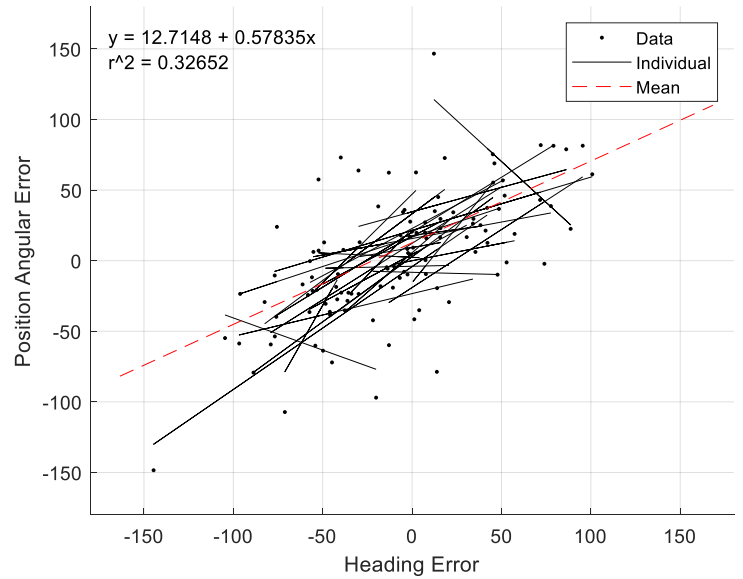


Figure 9. Scatter plots of position angular errors ( $\pi$ ) and heading errors ( $\eta$ ) in the Path-Integration condition, when  $L2/L1 = 2$  (A),  $L2/L1 = 1$  (B), and  $L2/L1 = 0.5$  (C) in Experiment 1. Each dot represents a pair of heading errors and position errors for one path and one participant. Each solid line is the regression line across paths for each participant. The dashed line is the mean regression line using the mean slope and intercept across participants.

A



B



C

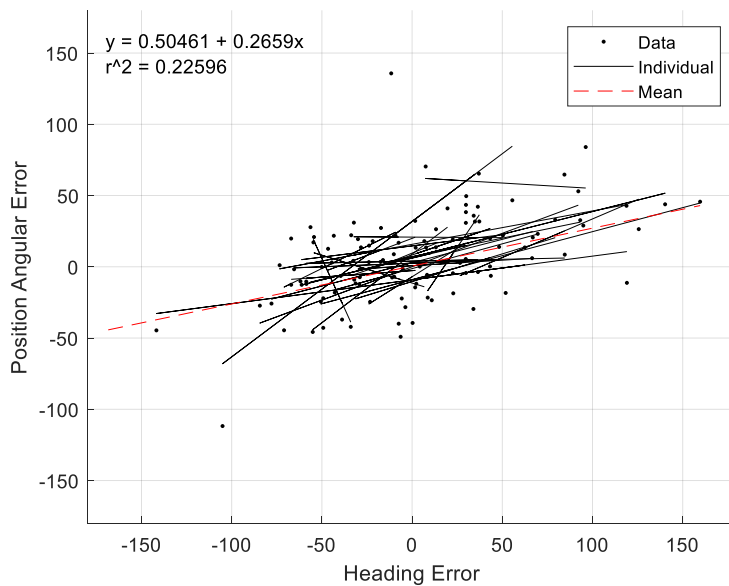


Figure 10. Mean SDs of homing errors ( $\theta$ ) observed and predicted by the self-localization hypothesis in the Path-Integration (PI), Landmark (LM), Both, and Conflict conditions, when the leg ratio (L2/L1) is 2 (A), 1 (B), and 0.5 (C) in Experiment 1. Error bars represent  $\pm 1$  SE without removing the variance from the individual difference.

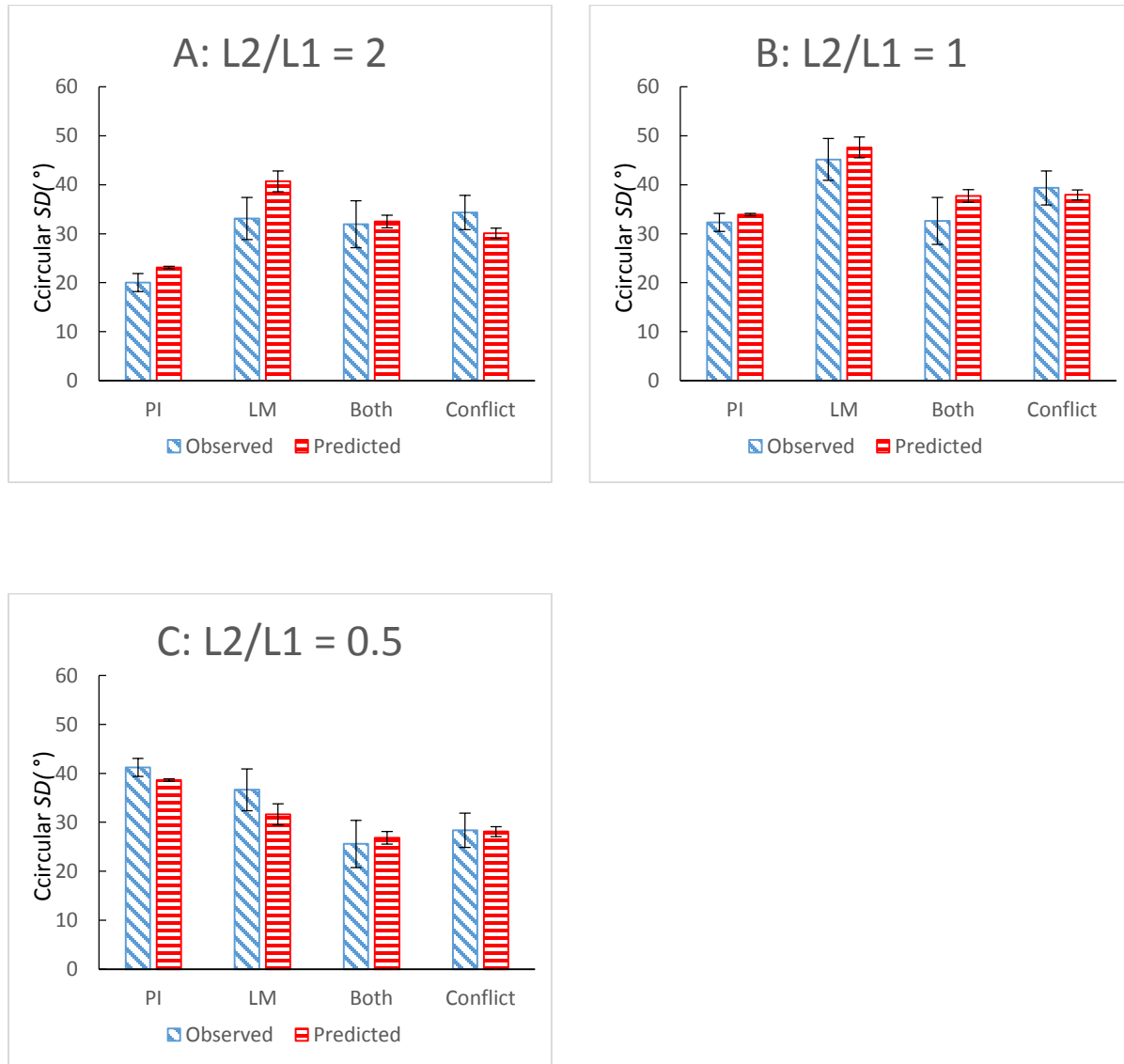


Figure 11. Mean observed SDs of the homing angular errors ( $\theta$ ) in the Path-Integration (PI), Landmark (LM), Both, and Conflict conditions, the optimal prediction by the Bayesian combination model (Optimal) in Experiment 2. Error bars represent  $\pm 1$  SE.

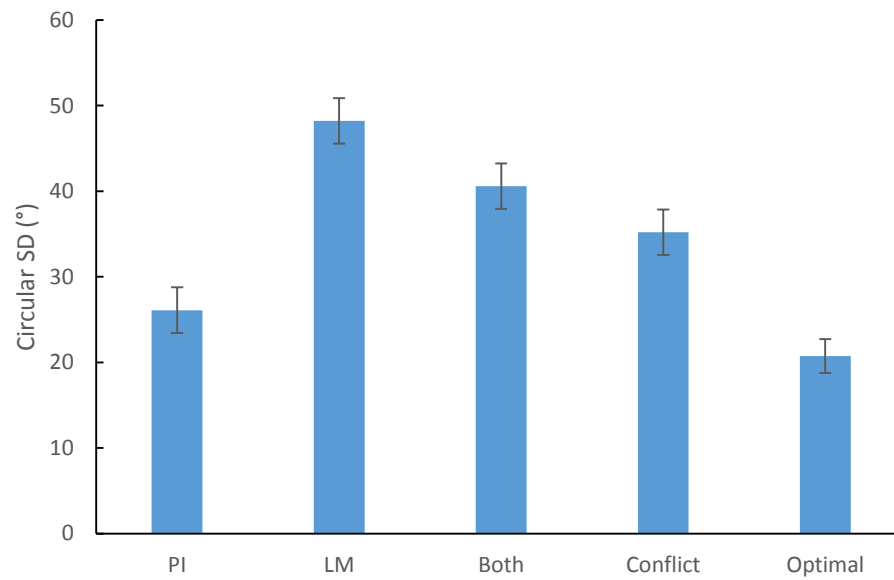


Figure 12. Mean observed SDs of the homing angular errors ( $\theta$ ) in the Path-Integration (PI), Landmark (LM), Both and Conflict conditions, the optimal prediction by the Bayesian combination model (Optimal) in Experiments 3 and 4. Error bars represent  $\pm 1$  SE.

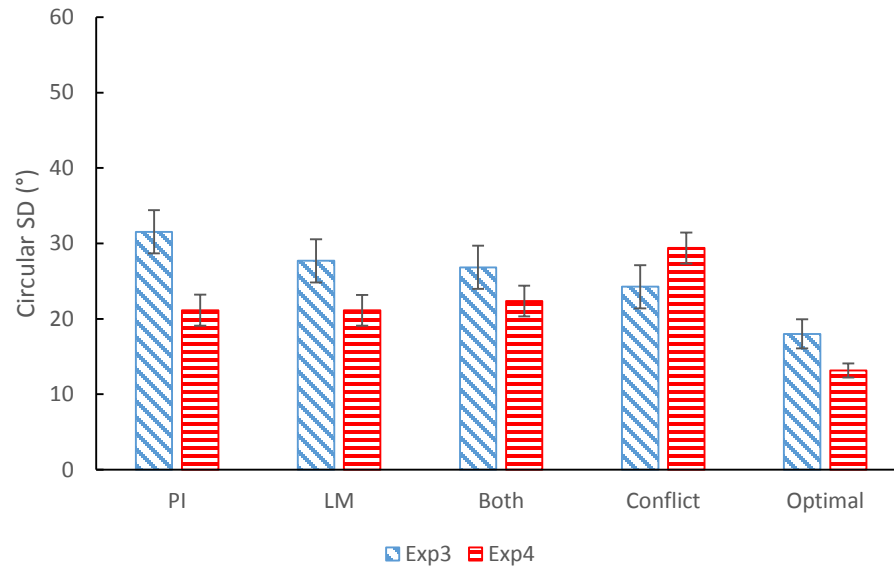


Figure 13. Mean observed SDs of the heading errors ( $\eta$ ) in the Path-Integration (PI), Landmark (LM), Both, and Conflict conditions, the optimal prediction by the Bayesian combination model (Optimal) in Experiments 3 and 4. Error bars represent  $\pm 1$  SE.

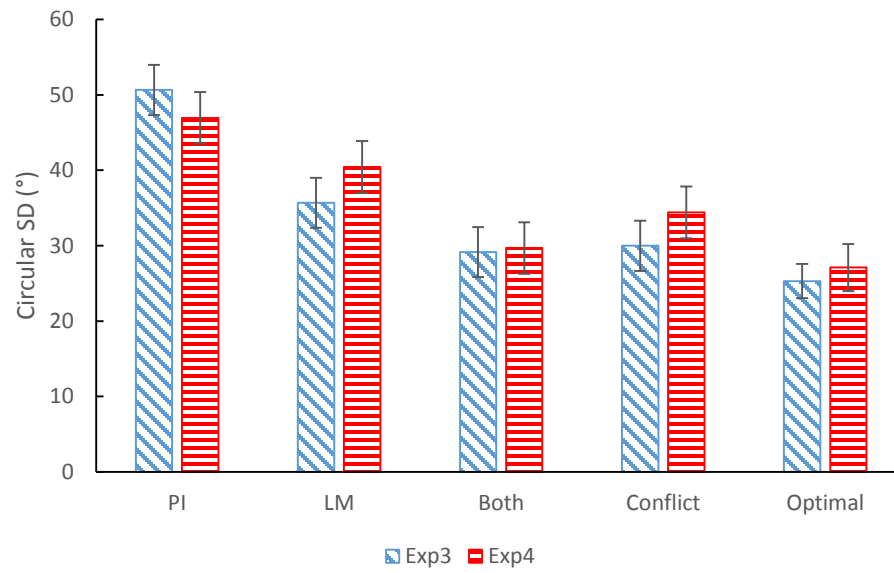


Figure 14. Mean observed SDs of the position angular errors ( $\pi$ ) in the Path-Integration (PI), Landmark (LM), Both, and Conflict conditions, the optimal prediction by the Bayesian combination model (Optimal) in Experiments 3 and 4. Error bars represent  $\pm 1$  SE.

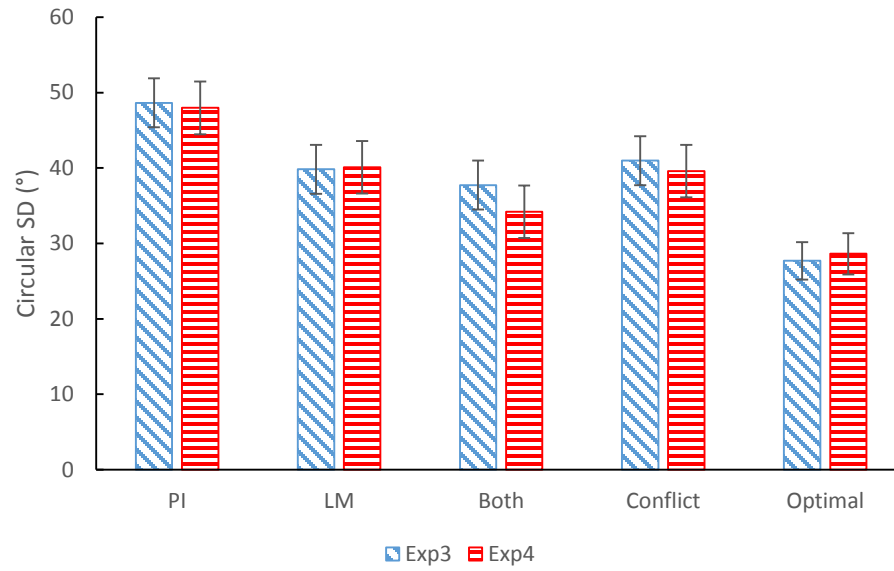
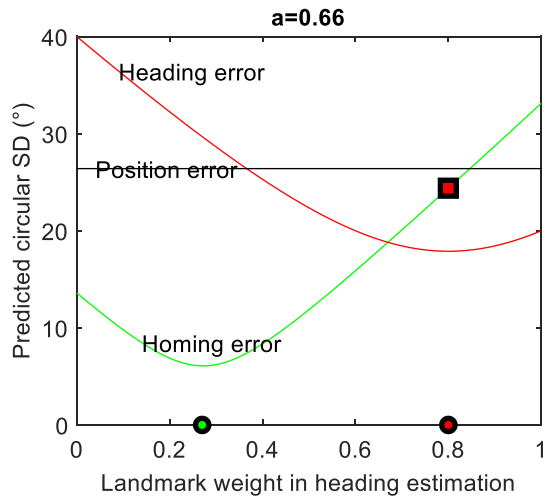
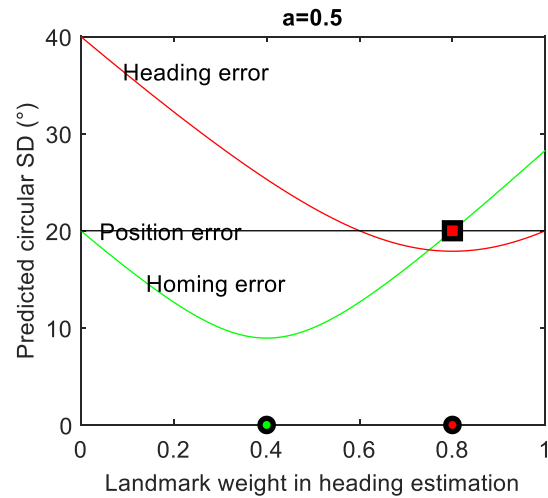


Figure A1. Simulation based on the equations in Table A1B. Predicted standard deviation (SD) of heading errors ( $\eta$ , the red line), position angular errors ( $\pi$ , the black line), and homing errors ( $\theta$ , the green line) in the Both/Conflict conditions as a function of the landmark weight used in combining heading estimates (*i. e.*,  $W_{\eta LM}$ ). We set  $\sigma_{\eta LM} = 40$ ,  $\sigma_{\eta PI} = 20$ , and  $\sigma_{ue} = 0$ . Slope  $a$  of the linear relationship of the position error and the heading error ( $\pi = a \times \eta$ ) from path integration is set to be 0.66 (A), 0.5 (B) or 0.33 (C). The green dot and red dot on the x axis are  $W_{\eta LM}$ s that lead to the minimum SD of homing ( $\sigma_{\theta}$ ) and heading errors ( $\sigma_{\eta}$ ), respectively. Note that the values of the red dots are always 0.8, whereas the value of the green dots varies. The distance between the green and the red dots increases with the value of slope  $a$  (*i. e.*,  $a \times 0.8$ ; see equation A5). The red square on the green curve denotes the predicted SD of homing errors ( $\sigma_{\theta}$ ) corresponding to the  $W_{\eta LM}$  that produces the minimum SD of heading errors ( $\sigma_{\eta}$ ).

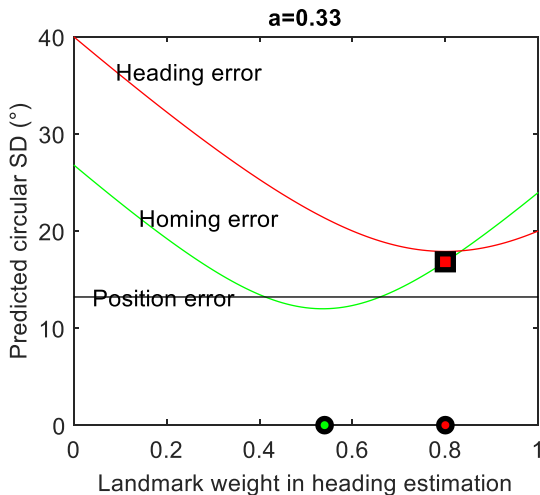
A

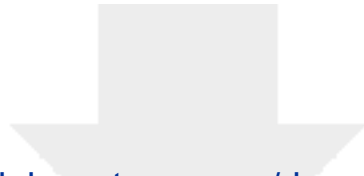


B



C





Click here to access/download  
**Supplemental Material**  
suppli20190731.docx

